12-2004

CBCT Panoramic Images vs. Traditional Panoramic Radiographs

Sunny Young Hutchinson

Recommended Citation

LOMA LINDA UNIVERSITY
Graduate School

CBCT Panoramic Images vs. Traditional Panoramic Radiographs

by

Sunny Young Hutchinson
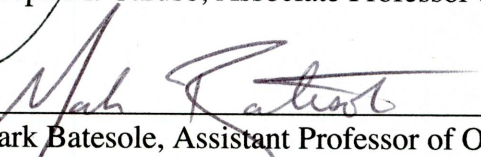
A Thesis submitted in partial satisfaction of
the requirements for the degree of
Masters of Science
in Orthodontics and Dentofacial Orthopedics
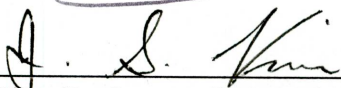
December 2004

Each person whose signature appears below certifies that this thesis in his opinion is adequate, in scope and quality, as a thesis for the degree Masters of Science.

, Chairman

Joseph M. Caruso, Associate Professor of Orthodontics

Mark Batesole, Assistant Professor of Orthodontics

Jay Kim, Professor of Biostatistics

Leroy Leggitt, Associate Professor of Orthodontics

ACKNOWLEDGEMENTS

CONTENTS

LIST OF TABLES

LIST OF FIGURES

LIST OF APPENDICES

ABSTRACT OF THE THESIS

CBCT Panoramic Images vs. Traditional Panoramic Radiographs

by

Sunny Young Hutchinson

Master of Science, Graduate Program in Orthodontics and Dentofacial Orthopedics
Loma Linda University, December 2004
Dr. Joseph M. Caruso, Chairman

The purpose of this research was to compare the accuracy of angular measurements of the panoramic image of the Newtom 9000™ Cone Beam Computed Tomography (CBCT) with the Sirona™ Orthophos panoramic unit. The study was separated into three parts: phantom study, patient study, and archform study. The phantom study used fabricated phantom typodonts to compare angular measurements between the Newtom 9000™ panoramic image and the Sirona™ panoramic radiograph. Accuracies of the measurements were then determined by comparing the values to the actual phantom typodont. No marked differences in angular measurements were recorded for the phantom typodont using either of the two imaging systems. Errors in fabricating the phantom typodont contributed to the results obtained.

For the patient study, retrospective angular measurements were made using previously taken panoramic radiographs and Newtom 9000™ scans of 60 patients undergoing orthodontic treatment at Loma Linda University. The patient study demonstrated significant differences between the Newtom 9000™ and the Sirona™ measurements. In the maxilla, the area of greatest difference was in the cuspid-premolar region, and the area of least difference was in the anterior and posterior region. In the mandible, the area of greatest difference was in the posterior region and the area of least

difference was in the anterior region. Factors that contributed to these results include: 1) differences of head position, 2) bucco-lingual angulation of the roots, and 3) distortions inherent to panoramic radiographic imaging.

The archform study determined if arch width and arch depth had any correlation to the mesial-distal radiographic dimensional width of the first molar. The assumption was that patients with wider vs. narrower arch width, and shorter vs. longer arch depth would have a diminution in radiographic image dimensions. Research was conducted using 41 sets of models from 60 patients used for the second part of this study. Results showed no correlation in arch width to radiographic molar width. A possible explanation for these results could be the temple caliper device on the Sirona™ panoramic unit. The device automatically adjusts the trough size according to patient skull size, thereby eliminating any existing correlation. For arch depth to molar dimensional width correlation, there was a statistical correlation on the left side of the arch only. One possible explanation is due to improper head positioning in the head holder of the panoramic unit. When this occurs, the midline of the patient is slightly turned to one side, resulting in magnification on that side.

Linear dimensional measurements of the mandibular first molars were then compared between the Newtom 9000™ panoramic image and the Sirona™ panoramic radiograph to the patient model to determine the dimensional accuracy. The dimensional measurements of the Newtom 9000™ were statistically similar to the model measurements. It was therefore concluded that the Newtom 9000™ dimensions, including angular dimensions, are much more accurate than those of Sirona™ angular dimensions.

CHAPTER ONE

INTRODUCTION

Accurate dental positioning improves alignment and occlusal stability and is

crucial for stable orthodontic treatment results. According to Mayoral, root parallelism

and proper mesial-distal root angulation is necessary for correct alignment in the apical

base and also for normal occlusion of the upper and lower teeth.[1] Moreover, Jarabak et al

state that if the roots are not parallel in teeth adjacent to an extraction site, the occlusal

load produces a rotational force that may result in distal canine rotation and mesial

inclination of the posterior teeth.[2] Jarabak et al also recognize that improper parallelism

could contribute to periodontal issues in patients with poor oral hygiene.[2]

Orthodontists commonly rely on panoramic radiographs to assess root parallelism

and mesial-distal angulation. The panoramic nature of this radiograph has allowed one to

visualize a large anatomic area, which has led to its popularity. Other advantages of this

technique include ease and speed of use, patient comfort and a relatively low radiation

dose.[3] The main disadvantage to the panoramic radiograph are the image distortions

created by this technique.[4] Such distortions limit the diagnostic capabilities of this

radiograph. For this reason, the panoramic radiograph is used only as a screening tool for

gross diagnosis in orthodontic treatment. Quintero et.al state:

> "It must be stressed, however, that panoramic radiography has
> many shortcomings related to the reliability and accuracy of size, location,
> and form of the images created. These discrepancies arise because the
> panoramic image is made by creating a focal trough or region of focus
> within a generic jaw form and size. The best images are obtained when
> the anatomy being imaged approximates this generic jaw form."[4]

There are two projections that create the focal trough or image layer in panoramic

radiography: 1) vertical and 2) horizontal.[5] The vertical component of the image layer,

like most conventional radiographic projections, is a result of the tube to target distance serving as the functional focus of the projection. The horizontal component of the image layer is created with the beam's center of rotation as its functional focus of projection. The functional focus of projection is affected by the rotation plane of the equipment and the rotation center, whether stationary or moving.[5,6,7,8] McDavid et al have shown that the dimensional width of the image layer in the anterior region ranges from 4.5-12 mm and is two to three times wider in the molar region.[9] The width of the image layer depends on a number of factors, such as the beam width and the speed of the film. As the beam width decreases, the image layer increases. Also, as the speed of the film decelerates, a narrowing of the image layer occurs, thus shifting the layer towards the center of rotation occurs. At the center plane of the image layer the magnification factors, in both the horizontal and vertical dimensions, are identical.[10,11] Diminution or magnification may occur, depending on whether the object outside of the central plane of the image layer is toward the film or toward the tube, respectively.[12,13]

Outside of the central plane of the image layer, each projection can create a separate magnification distortion.[14,15,7] For example, an asymmetric arch form results in magnification distortions due to discrepancies between the trough size and the object size. Additional magnification may occur in the horizontal projection due to film speed.[16,7] Magnification and distortion may also be caused by aberrant radiographic factors, such as improper head positioning, occlusal canting, patient movement, etc.[17] As a result of discrepancies between the magnification from both projections, McKee states that angular distortions can occur.[18]

There are several factors that can misrepresent the true mesial-distal root angulation on a panoramic radiograph. Philipp and Hurst recognized that the cant of the occlusal plane affected the parallelism and axial relationship of adjacent teeth.[19] Research has demonstrated that any change in inclination of the teeth in the bucco-lingual plane would be recorded as a change in the mesio-distal angulation.[20] Other investigators have shown that greater error occurred at increased lingual inclination. It has also been established that an inclined line in an object would be projected as a curved line in the image.[6]

Several other studies illustrated on average up to five degrees of inaccuracy in the mesial-distal angulation of adjacent teeth.[10] Interestingly, a common finding in many studies was that the locations with the highest incidence of distortion were the cuspid and premolar regions of both the maxillary and the mandibular arches.[21,22] McKee et al showed that there was over-divergence of the maxillary roots between the cuspid and first premolar and underestimation of the true angle in the mandibular dentition.[18]

Most patients with extreme crowding are treated by extraction of premolars. These areas are especially prone to relapse and thus accurate bracket placement is necessary for proper alignment.[23] Accordingly, Samawi has noted that one should be cautious when interpreting the axial relationship of the cuspid-premolar area and that application of angular measurements in that area should be avoided. This was especially true when there was an alteration in anterior head tilt or changes in inclination of the teeth in the bucco-lingual plane.[22] For an ideal image projection, the angle of the beam to the image layer should be close to 90 degrees. There is a marked deviation from the 90

degree orthoradial projection in the premolar region.[12,24] Furthermore, overlap within the dentition is the most apparent in the premolar area.[6]

A newer CT technology, the Newtom 9000™ (Quantitative Imaging, Verona, Italy), has been shown to produce images with minimal distortions, while sharing many advantages with the panoramic method, such as large visual anatomic field, patient comfort and ease of use. Ziegler et al state:

> "The Newtom 9000™ is a cone beam CT machine that can produce images in axial, paraxial, panoramic and in three-dimensional views. The machine produces CT quality images with a radiation dose comparable to a panoramic radiograph. The initial data is obtained by rotating the x-ray tube and image intensifier through 360 degrees around the stationary patient. One separate image is obtained per degree and in one cycle (76 seconds) a symmetric volume 10 cm in height and 12 cm in diameter is captured."[25]

In recent years, general public awareness of potential health risks from excessive radiation exposure has created reticence toward medical and dental radiography. A marked benefit of the Newtom 9000™ is that it possesses similar data acquisition capabilities as computed tomography units, but with lower radiation exposure to patients. Indeed, current investigations show that the amount of radiation exposure from a Newtom 9000™ scan is equal to between two and six panoramic radiographs.[26,16] Another study states that the patient receives an absorbed dose similar to a conventional full mouth periapical survey.[27]

Other factors that make the Newtom 9000™ a valuable diagnostic tool include its software capabilities for quantifying linear and angular measurements. Another benefit is that a single Newtom 9000™ scan produces a volumetric image which would allow the user to create two-dimensional views.

Additionally, the image reconstructive properties and dimensional accuracies have made the Newtom 9000™ a useful tool in oral surgery and implantology.[28] In orthodontics, common applications of the Newtom 9000™ include visualizing impacted teeth, assessing temporomandibular joints, assessing pathology, and evaluating the nasopharyngeal airway.[29,30]

Due to distortion effects, linear and angular measurements of panoramic radiographs, are inaccurate. One the other hand, the Newtom 9000™ has been shown to be dimensionally accurate, although accuracy in angular dimensions have not yet been determined.[29,30] Moreover, the Newtom 9000™ CBCT unit has the capability to create a similar panoramic view, without distortion effects. Although accuracy in angular dimensions is yet to be determined, the Newtom 9000™ has been shown to be dimensionally accurate. It is therefore the purpose of this study to compare the accuracy of angular dimensions from the panoramic views of the Newtom 9000™ to the panoramic radiograph of the Sirona™ Orthophos unit (Sirona Dental Systems, Bensheim, Germany).

CHAPTER TWO

MATERIALS AND METHODS

Materials and Methods Summary

Part I of this chapter outlines the fabrication and measurement of the phantom typodonts, which allow a comparison of angular measurements of the Sirona™ and the Newtom 9000™ unit from an ideal control. This section describes patterns of distortion between the two methods. Part II of this chapter identifies how image reconstruction and measurements were performed on previously taken records of orthodontic patients. The angular measurements of both the Newtom 9000™ panoramic images and Sirona™ panoramic radiographs were compared to identify differences between them. Part III of this chapter addresses the assumption that patients with narrower arch widths, or longer arch depth, produced increased image magnification, and the opposite effect for wider arch width and shorter arch depth. Correlations between the molar width to both arch width and arch depth were determined. Additionally, the linear dimensional magnification of the mandibular molar widths registered by the Newtom 9000™ and the Sirona™ images to patient models were compared.

Part I: Phantom Study

Fabrication

The purpose of the first part of the study was to create phantom typodonts with pentamorphic normal arch forms and parallel dentition. The typodonts were constructed using radiopaque PVC plastic pegs to represent the dentition. Each arch was fabricated with twelve pegs to represent the number of teeth from first molar to the opposite first molar. The length of each peg was 25 mm, and was either 7 mm or 10 mm in diameter.

Centrals, cuspids and first molars were 10mm in width and the laterals, first premolar and

second premolars were 7 mm. Each peg had a 1 x 1 x 1 mm divet in the center of both

ends plugged with amalgam to create radiographic landmarks for ease of measuring

dental angulations. Pentamorphic normal template design was copied onto plastic sheets

in which the plastic pegs were individually bonded and placed 2 mm (Fig. 1). Sheet

dimensions were 5 x 5 inches x 1.5 mm thick.
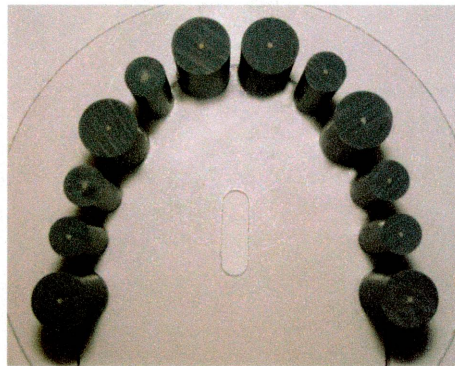
Fig. 1. Zero Degree Phantom Typodont (occlusal view).

Next, one sheet was placed on the other to represent the full maxillary and mandibular

dentition. The sheets were held together and suspended in a clear plastic container by a

screw-in rod attached to the lid, and a container was used to hold the typodont in a

suspended gelatin matrix in order to obtain proper x-ray attenuation (Fig. 2). Two sets of

dentitions were then fabricated. The first set was created with pegs set at 0 degrees from

a line perpendicular to the occlusal plane (Fig. 3A). The second set was created using

pegs with slanted ends, giving a 10 degree mesial-distal angulation from a line

perpendicular to the occlusal plane (Fig. 3B).
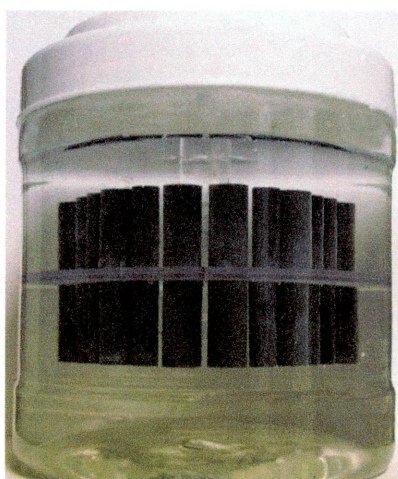
Fig. 2. Attenuation Container. Phantom typodont inside gelatin matrix.
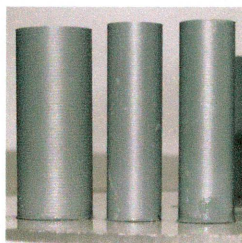
Fig. 3A. 0 Degree Pegs (lateral view).   Fig. 3B. 10 Degree Pegs (lateral view).

Newtom 9000™ Measurements

Newtom 9000™ scans were performed on both the 0 degree and 10 degree

phantom typodonts. For each scan, the phantom typodont was suspended in the

attenuation container and placed on the Newtom 9000™ bed with the midline centered

and occlusal plane set perpendicular to the floor. Primary reconstruction of the raw

image was done with the axial sections set 1mm apart and parallel to the referenced

occlusal plane. The plastic sheets between the maxillary and mandibular arches

represented the occlusal plane. In order to determine the angulations of the typodont

pegs from a panoramic view, a secondary reconstruction was done. The maxillary and

mandibular arches were then measured separately. From the reference occlusal plane

position, the axial reference line was scrolled up in 1 mm increments through the axial

sections towards the maxillary arch or down towards the mandibular arch. The first axial section capturing all 12 radiographic amalgam points established the reference occlusal plane (Fig. 4).
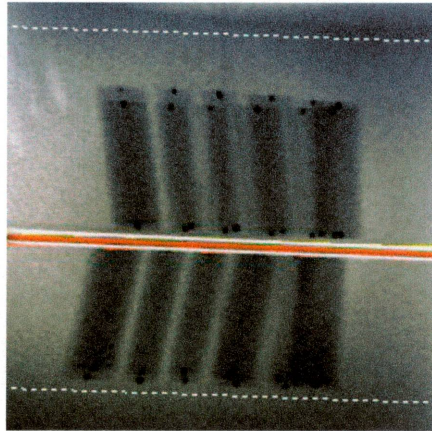
Fig. 4. Phantom Occlusal Plane. Red center line - representing occlusal plane.

In order to begin the secondary reconstruction, panoramic parameter setups were selected. The thickness chosen was 10 mm. This was a good balance between visualizing most of the dentition, but not so thick as to reduce the clarity of the image. However a consequence was that with each increase in slice thickness there corresponded a decrease in image clarity.

From the reference occlusal view, the panoramic image was created by connecting the radiographic points along the arch (Fig. 5).
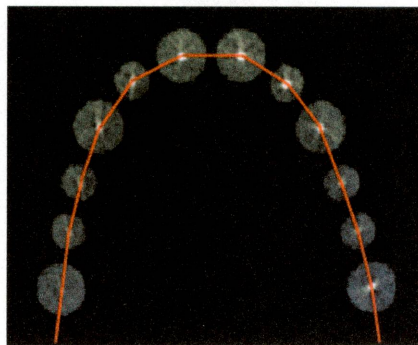
Fig. 5. Reference Occlusal View.
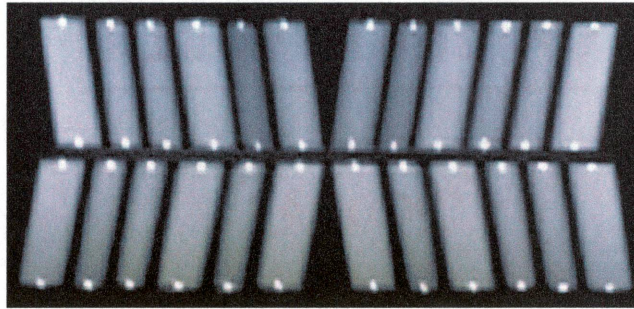
Fig. 6. Full Newtom 9000™ Panoramic View of the Ten Degree Dentition.

This produced a panoramic image visualized orthoradially from the selected path (Fig. 6).

For ease of visualization and measurement accuracy, the "line" tool was used to draw a

line connecting the radiographic points on each end of the peg in the panoramic

projection. Then, using the "angle" tool, the angle was measured from the line

connecting the two radiographic points to a line perpendicular to the occlusal plane (Fig.

7 and 8). All measurement data was recorded on an Excel™ spreadsheet (Microsoft

Excel X).
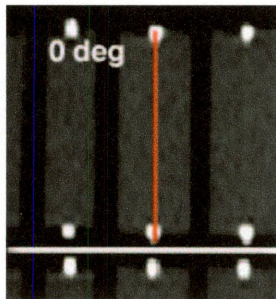
Fig. 7. Long Axis Line.
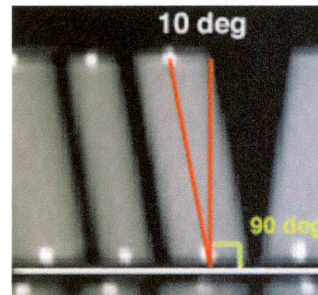
Fig. 8. Phantom Typodont Angular Measurement.

Sirona™ Measurements

The Sirona™ Orthophos DS panoramic unit used for this study was set at 15 mA,

69 kVP, and at 14.1 seconds for each exposure. To minimize potential error factors, the

caliper for the temple support was set in a constant position. The attenuation container

housing the phantom was placed on an adjustable stand that permitted the occlusal plane

to be set parallel to the floor. In order to position the dentition in the focal trough, the

maxillary pegs representing the incisors were placed in the area of the groove of the bite stick. The midline indicator light was then used to center the phantom in the headrest. Settings were repeated for all subsequent testing of the phantoms.

Angular measurements were performed using the "angle" option tool available on the Sirona™ imaging computers. Using a line perpendicular to the occlusal plane as the reference plane, the angle was measured to the line connecting the two radiographic points on each peg. The maxillary and mandibular arches were measured separately. All data was recorded on an Excel™ spreadsheet.

Part II: Patient Study

Patient Selection

For this portion of the study, pretreatment records of 60 orthodontic patients, undergoing treatment at Loma Linda University orthodontic clinic, were selected. The inclusion criteria for selection of patients required: 1) that the patients had the Newtom 9000™ scan and the Sirona™ panoramic radiograph taken on the same day, 2) that the panoramic radiograph and the reconstructed Newtom 9000™ image were visually clear enough to discern the pulpal canal of the roots to enable accurate measurements and 3) that all patients were in permanent dentition and had intra-arch dental alignment, such as minimal arch length deficiency and minor rotation. Selected subjects were de-identified using numeric codes in order to comply with HIPAA regulations and to avoid subjective interpreter errors.

Newtom 9000™ Measurements

Primary reconstruction of all raw images were set 1 mm apart and the axial line parallel to the functional occlusal plane. The functional occlusal plane was defined as the

11

plane that best fit the cusp tips of functioning posterior teeth, which mainly included the premolars and the first molar.

In order to begin the secondary reconstruction for each patient, the occlusal plane was identified from the scout image (Fig. 9). To create a panoramic image, from the reference occlusal plane, the axial line was moved up 5 mm towards the maxilla or down 5 mm towards the mandible (Fig. 10). Due to the inclination differences in the patient's incisors, a height of 5 mm from the functional occlusal plane toward the maxilla or the mandible was chosen to increase the likelihood of remaining within the depth of the image facial-lingually. This made it possible to see as much of the root length as possible in order to appropriately measure the angle of the tooth. The panoramic image parameters were then set at 10 mm trough thickness (Fig. 11A and 11B),
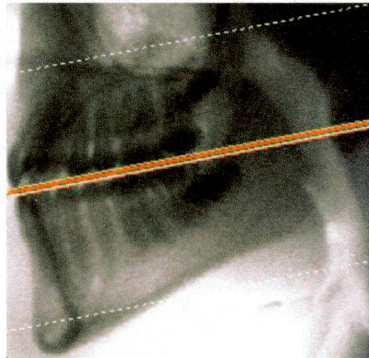
Fig. 9. Functional Occlusal Plane.
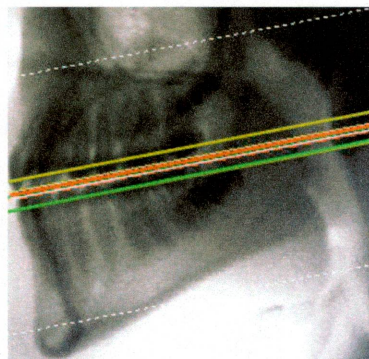
Fig. 10. Functional Occlusal Plane Modification. Yellow line/Green line represents 5mm above/below the functional occlusal plane.
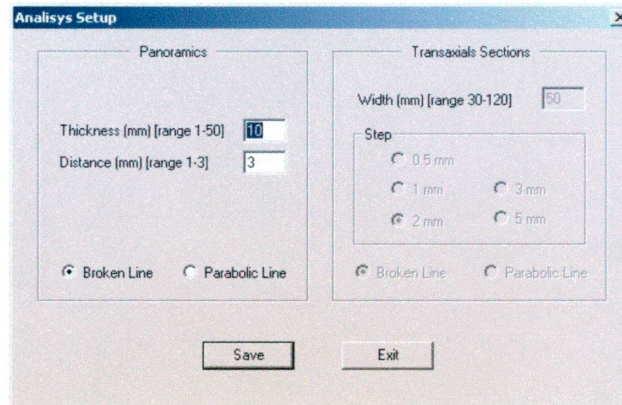
Fig. 11A. Newtom 9000^{TM} Parameter Setup Screen.
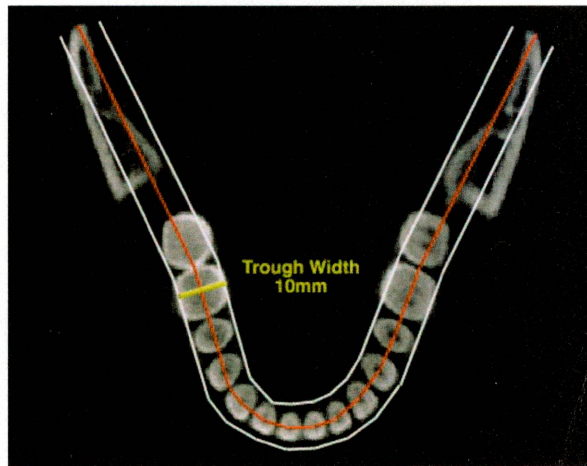
Fig. 11B. Trough Thickness. Trough width of 10mm created
from center line (red).

a factor more important in patients with decreased interincisal angle. From the chosen

axial occlusal view, landmarks were selected around the arch perimeter to create the

panoramic image. For the maxillary arch, the first point selected was the most posterior

point of the right condyle, followed by a point on the first molar that was the most distal

and most centered bucco-lingually; and then to a point on the mesial and most centered

bucco-lingually to the first premolar, next to the center of the pulpal canal of the cuspid,

followed lastly by the lingual surfaces of the lateral and central incisors. The lingual

surfaces of the lateral and central incisors were chosen due to the increased torque of

these teeth. The points continued to the opposite side using the same landmarks

described (Fig. 12 and 13). Creating a panoramic image on the mandibular arch followed the same method previously described for the maxillary arch, except for the points selected on the laterals and centrals. In those locations, instead of the lingual surfaces of the incisors, the centers of the pulpal canals were chosen due to the more upright nature of the teeth.
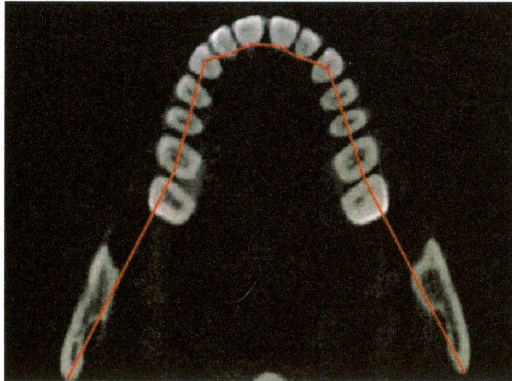
Fig. 12. Maxillary Occlusal Outline.   Fig. 13. Mandibular Occlusal Outline.
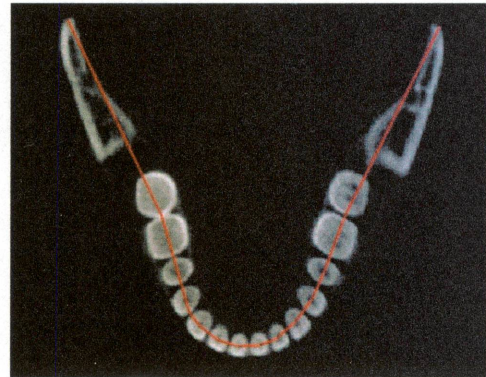
All panoramic images created on the computer screen were visualized with their sizes minimized. Hence, in order to appropriately determine root angulation, the panoramic image was magnified to 150% for better visualization. With the constructed panoramic image, angular measurements were performed using the "line" and "angle" software tools from the imaging computers of the Newtom 9000™ system.

All teeth were measured in the same manner, except the first molars. Angular measurement of the central incisors, lateral incisor, cuspid, first premolar and second premolar teeth were initially measured using the "line" tool to trace the cervical half of the root length of the pulpal canal which represented the long axis for each tooth. Next, with the "angle" tool, the angle for the root of each tooth were measured by superimposing the angle over the initial line traced to a plane perpendicular to the occlusal plane (Fig. 14). The apical half of the root was not used due to high incidences

of curvatures and variabilities, and teeth that did not have discernable pulpal canals radiographically due to multiple roots were eliminated from this study. First molars were measured differently due to the occurrence of high incidences of pulpal canal obscurity from multiple roots. Initially, molar measurements were made by creating a line tangent to both the contour of the clinical crown and to the mesial surface of the root. The angle was then determined by measuring that line to a line perpendicular to the occlusal plane (Fig. 15).

Fig. 14. A) Long Axis of Root. For the central incisor, lateral incisor, cuspid, first premolar and second premolar, a line was drawn over the pulpal canal of the cervical half of the root, representing the long axis of the root. B) Angular Measurement. The angle of the root was measured by superimposing the initial line drawn to a plane perpendicular to the occlusal plane.

Fig. 15. A) Molar Line. Yellow line is tangent to the height of contour of the crown and the contour of the root. B) Molar Angle. The angle is measured from the molar line (red) to a line perpendicular to the occlusal plane (white).

The full dentition measurement is visualized below in Fig. 16. All data was entered on an Excel™ spreadsheet.
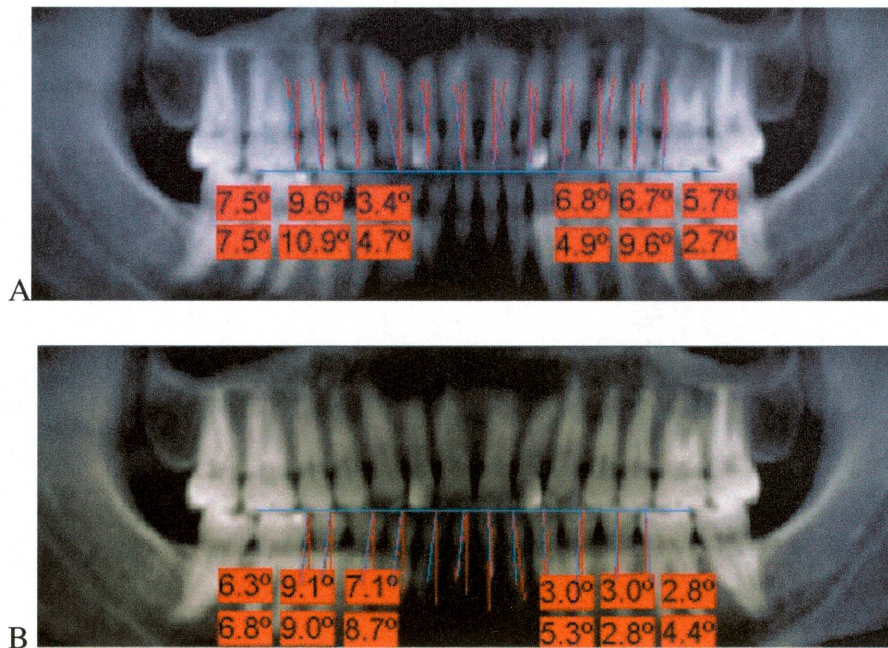
Fig. 16. (A) Full maxillary measurements. (B) Full mandibular measurements.

Sirona™ Measurements

Angle measurements on patients' panoramic images were performed using the same method as on the phantoms on the Sirona™ computer. Similar to Newtom 9000™ patient measurements, the occlusal plane was designated from the first molar to the opposite first molar. All data was recorded on an Excel™ spreadsheet.

Part III: Archform Study

Model Measurements

The purpose of this part of the study was to first determine if there was a correlation between mesial-distal width of the first molar to arch width or arch depth. It is known that objects across the image layer produce magnification or diminution of the image depending on whether the object is placed near to or away from the film, respectively. Therefore, the goal was to determine if patients with narrower jaws or arch width would be farther away from the film, resulting in image magnification or vice

versa. It was demonstrated that for most panoramic units, there is an increased magnification towards the posterior region. Therefore, a patient with longer arch depth should show increased magnification of the first molars than patients with shorter arch depth. Only 41 out of the 60 patients from the angulation study had existing diagnostic models, which used for this part of the study. The first molar widths on the models were measured using a caliper. Mesial-distal molar width on the Sirona™ panoramic radiograph was measured using the measuring tool in the Sirona™ computer (Fig. 17).

Fig. 17. Linear Measurement on the Sirona™.

For both the maxillary and the mandibular arch, the arch width was determined to be a linear dimension in the visual center of the alveolar ridge in the location of the mesial surface of the first molar to the mesial surface of the opposite first molar. For both the maxillary and the mandibular arch, the arch depth was determined to be a linear dimension from the incisal edge of the anterior teeth to a point bisecting a line tangent to the mesial surfaces of the first molars (Fig. 18). All data was recorded on an Excel™ spreadsheet.
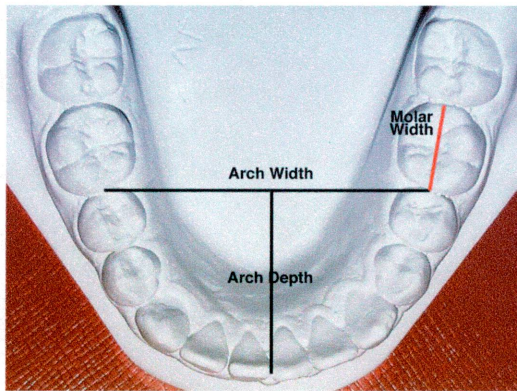
Fig. 18. Model: Arch Width and Arch Depth. Arch width and arch depth
are represented by the black lines. The mesial-distal dimensional molar width
Is represented by the red line.

This part of the study also compared the linear dimensional accuracy of the

mandibular first molars recorded by the Newtom 9000™ panoramic image and those

recorded by the Sirona™ panoramic radiograph to the diagnostic model of the patient.

Only 35 out of the 41 patients were used in this section due to the patients' Newtom

9000™ files being unavailable at the time of data collection. Measurements of the

mandibular first molars were taken from the Newtom 9000™ panoramic image and

compared with the existing measurements of the model and Sirona™ from the first

section of this part of the study (Fig. 19). All data was recorded on an Excel™

spreadsheet.
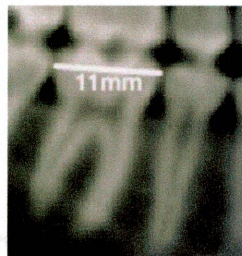
Fig. 19. Linear Measurement on the Newtom 9000™.

18

Statistical Methods

For the phantom study, angulations were measured from the Newtom 9000™ and the Sirona™ panoramic unit to the phantom typodont. A comparative analysis was performed to evaluate if angular measurements were within +/-2 degrees from each other.

For the patient study, angulation measurements for each of the 24 teeth were performed between Newtom 9000™ panoramic images and the Sirona™ panoramic radiographs. Descriptive statistics were defined to determine the mean absolute angular differences and the standard deviations for each of the teeth. Wilcoxon Signed Rank Test was performed to determine the statistical significance of the angular differences between the two methods. Intraclass Correlation Coefficient (ICC) was calculated to determine the reliability of the measurements.

For the archform study, Pearson Correlation Coefficient was performed to determine the strengh of a relationship between the mesial-distal dimensional width of the first molar to arch width and arch depth. Additionally, percent error in magnification were calculated to determine linear dimensional accuracy of the first molar dimensional width between each of the Newtom 9000™ and the Sirona™ images and the actual patient models.

CHAPTER THREE

RESULTS

Phantom Study

All measured values fell within +/-2 degrees between the phantom typodont, Newtom 9000™, and the panoramic radiographs. Refer to Appendix IV.

Patient Study

From data acquired for sixty patients, the descriptive statistics were defined and the mean absolute angular differences were plotted from right to left, with the maxilla and the mandible on separate plots. The mean absolute differences were used for each tooth to determine the total difference in degrees between the two methods.

In the maxilla, the largest differences were in the cuspids and first premolars and the lowest values were in the molars and central incisors. For the mandibular arch, the largest differences were in the first molars, which declined toward the midline. The differences were higher on the right side than on the left side, except for the mandibular right first premolar, which was valued at 4.8 degrees. This was lower when compared to the left first premolar at 5.1 degrees (Table 1 and Figure 20). For actual data measurements, refer to Appendix I.

	Right 1st Molar	Right 2nd Premolar	Right 1st Premolar	Right Cuspid	Right Lateral	Right Central	Left Central	Left Lateral	Left Cuspid	Left 1st Premolar	Left 2nd Premolar	Left 1st Molar
Mx	5.3	9.8	10.7	14.2	9.2	6.7	4.3	5.8	10.0	8.7	6.9	5.1
Md	9.9	7.6	4.8	5.2	4.6	4.6	3.6	4.2	4.5	5.1	7.1	9.5

Note: All numerical values shown above are in degree values.

Table 1. Mean absolute angular difference between Newtom 9000™ and Sirona™ angles (n=60).
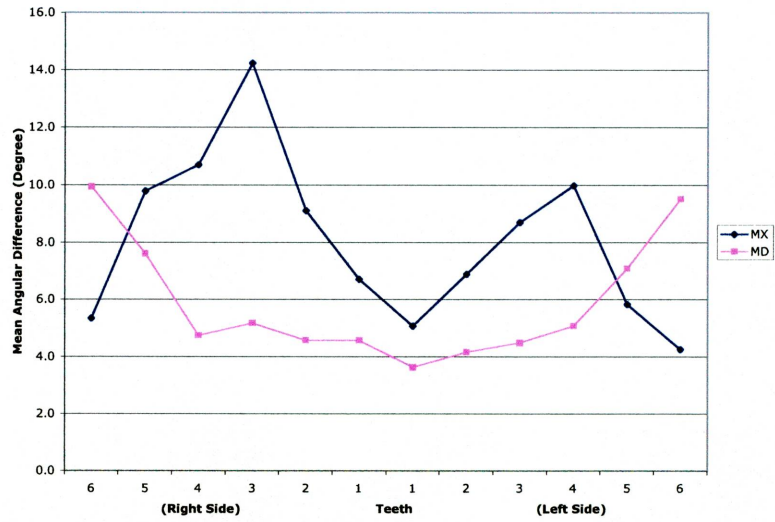
Figure 20. Mean absolute angular difference between Newtom 9000^{TM} and Sirona^{TM} angles.

The standard deviation values ranged from 4.3-14.2 degrees in the maxillary arch, and

3.1-5.2 in the mandibular arch (Fig. 21 and 22).
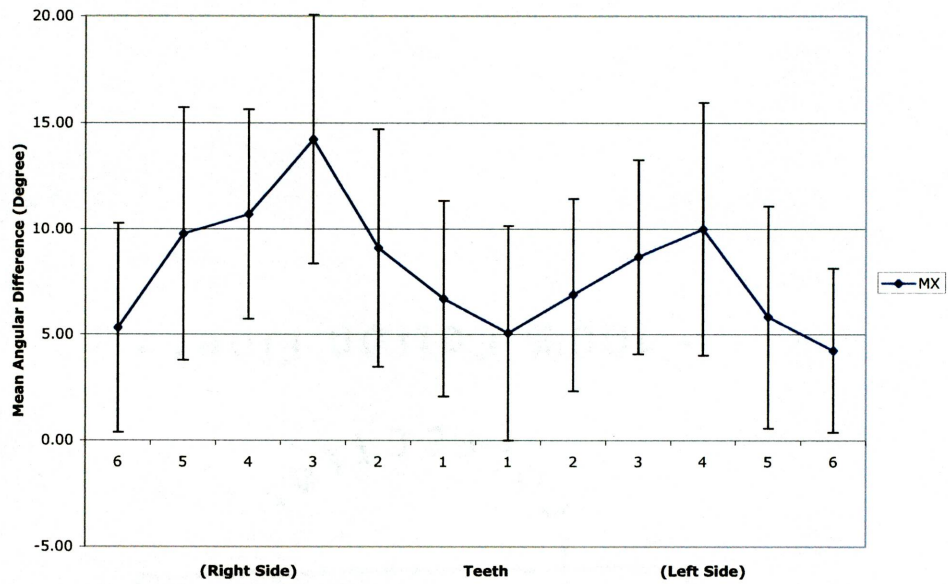
Figure 21. Maxillary mean angular differences with standard deviation.
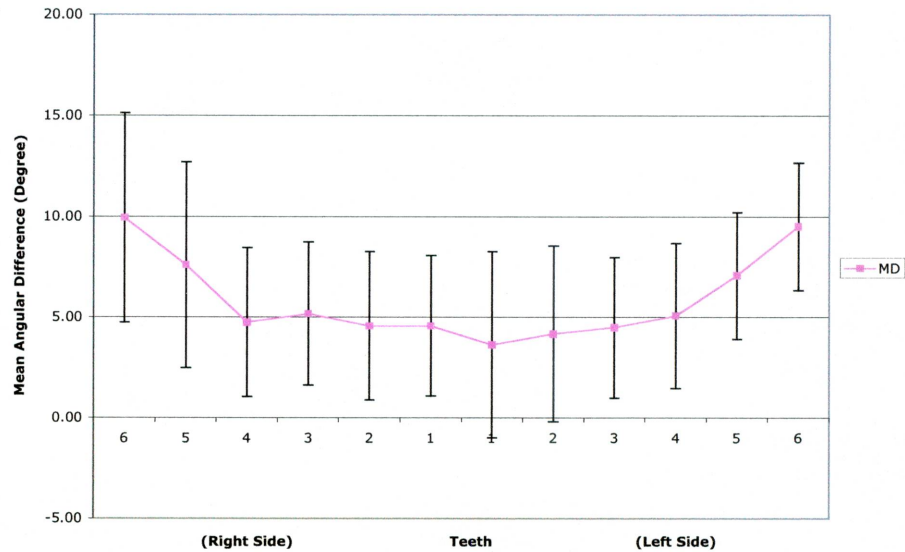
Figure 22. Mandibular mean angular differences with standard deviation.

Statistical significance of the angular differences between the Newtom 9000™ and the Sirona™ were also determined. There was significant variance in angular differences obtained by both methods for all teeth in the maxilla. In the mandible, the right cuspid and the left central, lateral and cuspid had similar angular measurements between the two methods. The remaining mandibular teeth had angular measurements that were significantly different (Table 2).

	Right 1st Molar	Right 2nd Premolar	Right 1st Premolar	Right Cuspid	Right Lateral	Right Central	Left Central	Left Lateral	Left Cuspid	Left 1st Premolar	Left 2nd Premolar	Left 1st Molar
Mx	0.0019*	<0.0001*	<0.0001*	<0.0001*	<0.0001*	<0.0001*	<0.0001*	<0.0001*	<0.0001*	<0.0001*	<0.0001*	0.0040*
Md	<0.0001*	<0.0001*	<0.0001*	0.3312	0.0007*	0.0017*	0.6120	0.4020	0.7541	0.0009*	<0.0001*	<0.0001*

Note: The asterisk "*" indicates statistical significance at the a=0.05 level

Table. 2. Statistical evaluation of angular measurements.

To determine intraclass reliability, every third consecutive patient was chosen from the list of 60 patients, totaling 20 patients. For each of the patients, angular measurements were taken on three separate occasions on the maxillary right first molar, maxillary left cuspid, mandibular right first premolar and mandibular left lateral, from

both the panoramic radiograph and the Newtom 9000™ image. Patient angles were rechecked using the intraclass correlation coefficient (ICC) to determine a reliability value of 98%. Refer to Appendix III.

Archform Study

From the patient model study, correlations were based on the p-value, with less than .05 as significant. There was no correlation (r=-0.128, p=0.426 and r=0.183, p=0.253) between the respective mean differences of the maxillary right and left first molars with the maxillary width. There was no correlation (r=-0.239, p=0.132 and r=0.013, p=0.938) between the respective mean differences of the mandibular right and left first molars with the mandibular width. There was no correlation (r=0.187, p=0.241) between the mean differences of the maxillary right first molar and maxillary depth; although there was a correlation (r=0.340, p=0.030) between the mean absolute differences of the maxillary left first molar and maxillary depth. There was no correlation (r=0.022, p=0.892) between the mean absolute differences of the mandibular right first molars and the mandibular depth, but there was a moderate correlation (r=0.423, p=0.006) between the mean absolute differences of the mandibular left first molars and the mandibular depth (Table 3). To see actual measurements, refer to Appendix II.

	maxillary width	mandibular width	maxillary depth	mandibular depth
right	r=-0.128 p=0.426	r=-0.239 p=0.132	r=0.187 p=0.241	r=0.022 p=0.892
left	r=0.183 p=0.253	r=0.013 p=0.938	r=0.340 p=0.030*	r=0.423 p=0.006*

(*) Represents statistical significance (less than 0.05).

Table 3. Statistical analyses of arch width and arch depth to molar width.

For the linear dimensional measurements of the mandibular molars, the Sirona™ values ranged from 9.1 to 38.1% magnification on the right side with an average of 23.3%. On the left side, the values ranged from 2.3 to 32.5% magnification with an average of 17.6%. For the Newtom 9000™, the values ranged from –2.7 to 9.1% magnification on the right side with an average of 1.5%. On the left side, the values ranged from –4.2 to 6.7% with an average of 1.2% (Table 4).

	right % magnification	average	left % magnification	average
Sirona™	9.1 to 38.1%	23.3%	2.3 to 32.5%	17.6%
Newtom 9000™	-2.7 to 9.1%	1.5%	-4.2 to 6.7%	1.2%

Table 4. Linear Dimensional Magnification.

CHAPTER FOUR

DISCUSSION

Phantom Study

All values for the phantom typodont measurements obtained for each of the Newtom 9000™ images and the Sirona™ panoramic radiograph were comparable to the actual phantom typodont values. This shows that parallel lines remain constantly parallel, at all angles they are viewed from. These findings can only be true for ideal archforms, which allows the parallel pegs to remain in the central plane of the image layer where projections in the horizontal and vertical dimensions are equal, and thus distortions are minimal.

Patient Study

The greatest mean differences between the Newtom 9000™ and the Sirona™ measurements in the maxilla were in the cuspid and premolar area. This agrees with most literature findings.[21,18,22] In this region, there was a marked deviation from the 90 degrees projection, and therefore greater distortion was likely to occur. Furthermore, the canine-premolar region was most susceptible to bucco-lingual root inclination, which would exaggerate the angular distortion in the mesio-distal direction.[22]

In the maxilla, the least amount of angular difference between the Newtom 9000™ and the panoramic radiograph was found in the incisor and molar region. The effective rotational center in the panoramic unit moved continuously along a path into three general areas. In the anterior and posterior areas, the beam was projected at 90 degrees to the image layer. Due to the orthoradial projection, the image quality in this area had minimal distortion (Fig. 23).
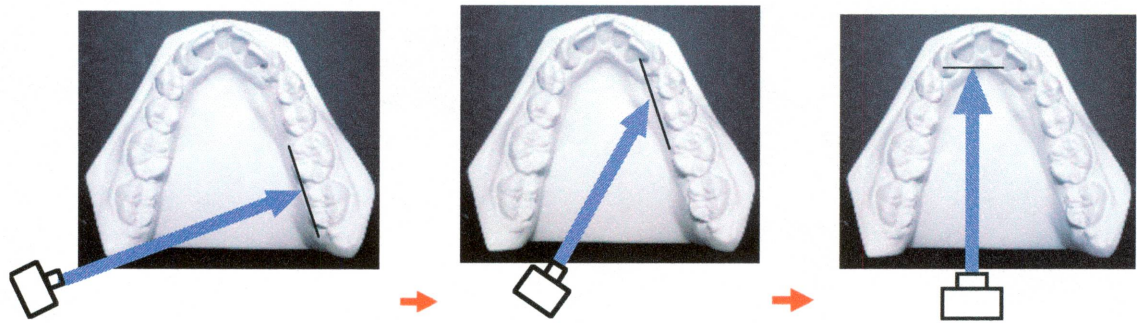
Fig. 23. Beam Projection. In the molar and anterior teeth, the beam projects at 90 degrees to them. In the cuspid and premolar areas, the beam deviates from the 90 degrees projection.

In the mandible, the least amount of angular difference was in the anterior region, and the greatest in the posterior region. There may be a combination of factors that could explain these results. For example, on many of the patients' panoramic radiographs, there were telltale signs pointing to patients having their head tilted slightly downwards during the exposure. Such signs include the hard palate being close to the apices of the maxillary teeth, excessive convergence of the maxillary roots, excessive divergence of the mandibular roots, and a severe curve of Spee (Fig. 24 and 25).
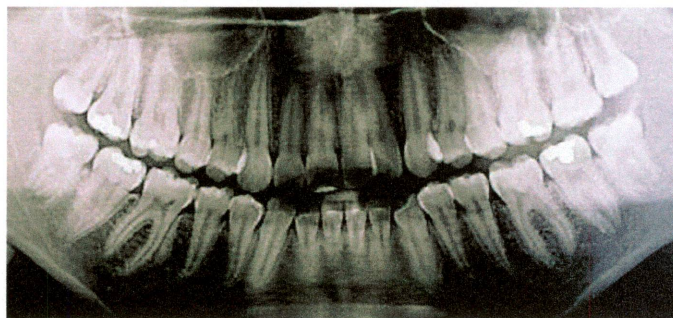
Fig. 24. Patient Head Tilt Effect. Panoramic radiograph with patient head tilted downwards.
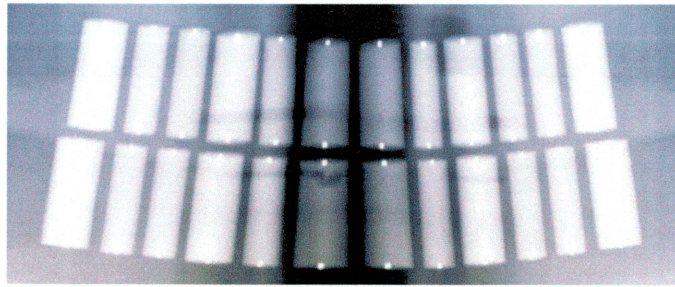
Fig. 25. Phantom Typodont Tilt Effect

Another contributing factor was the manner in which the x-ray beam diverged

towards the object. The beams in most panoramic units are directed upward toward the

patient at about 7-10 degrees[6] (Fig. 26). The divergent beam reached the maxilla at an

average of 15 degrees and reached the mandible at an average angle of approximately 5

degrees (Fig. 27).[31] This could have contributed to the respective excess of convergence

and divergence of the maxillary and mandibular teeth.
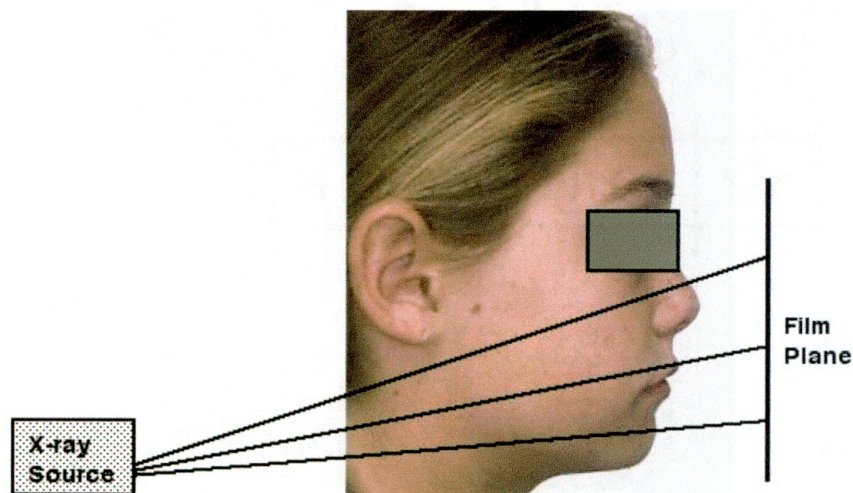
Fig. 26. X-ray Source Toward Film Plane. The X-ray beam directs upward
towards the film plane at an angle between 7-10 degrees[6].
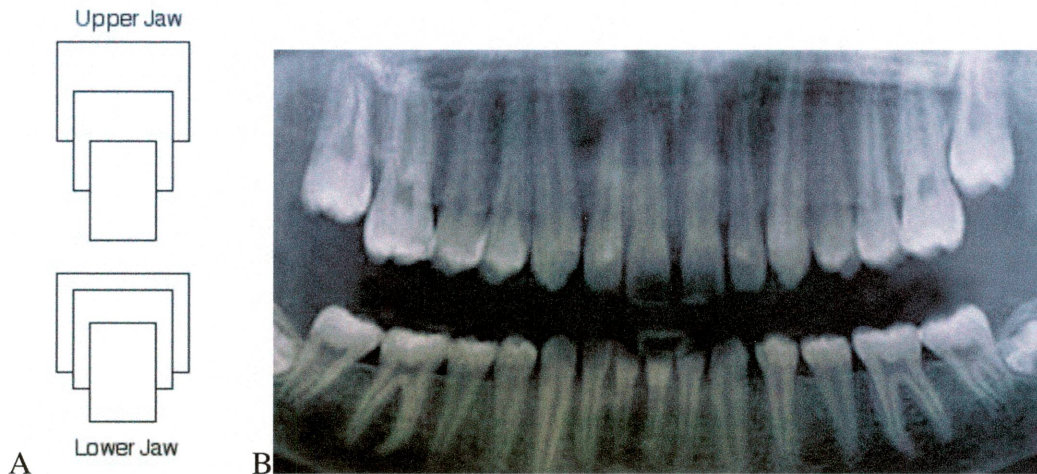
Fig. 27. Divergence of the X-ray Beam. (A) The divergence of the beam through the depth of the image layer creates the illustrated distortion effects (Modified from Langland et al[6]). (B) Panoramic radiograph modified through Adobe® Photoshop® Elements (2nd Ed.) illustrate elongation of the maxillary dentition and foreshortening of the mandibular dentition.

The method of occlusal positioning during radiographic exposure may have contributed to the observed angulation differences. In the panoramic unit, patients were positioned with their anterior teeth at an end-to-end position on the bite stick. If the patient had an excess curve of Spee in the mandible, biting on the bite stick may have increased the occlusal plane angle, which would therefore have increased the divergent effect of the mandibular teeth, particularly posteriorly.

In the Newtom 9000™, distortions from these factors are eliminated because the reconstructive capability of this machine allowed us to more accurately determine the functional occlusal plane, which produced a more accurate panoramic image and thus more accurate dental angulation (Fig. 28 A, B, C, D). The plane is based only on the patient's posterior occlusion in maximum intercuspation, and not dependent on patient positioning. Distortions caused by improper head position can be eliminated because the image is created from a volume data.
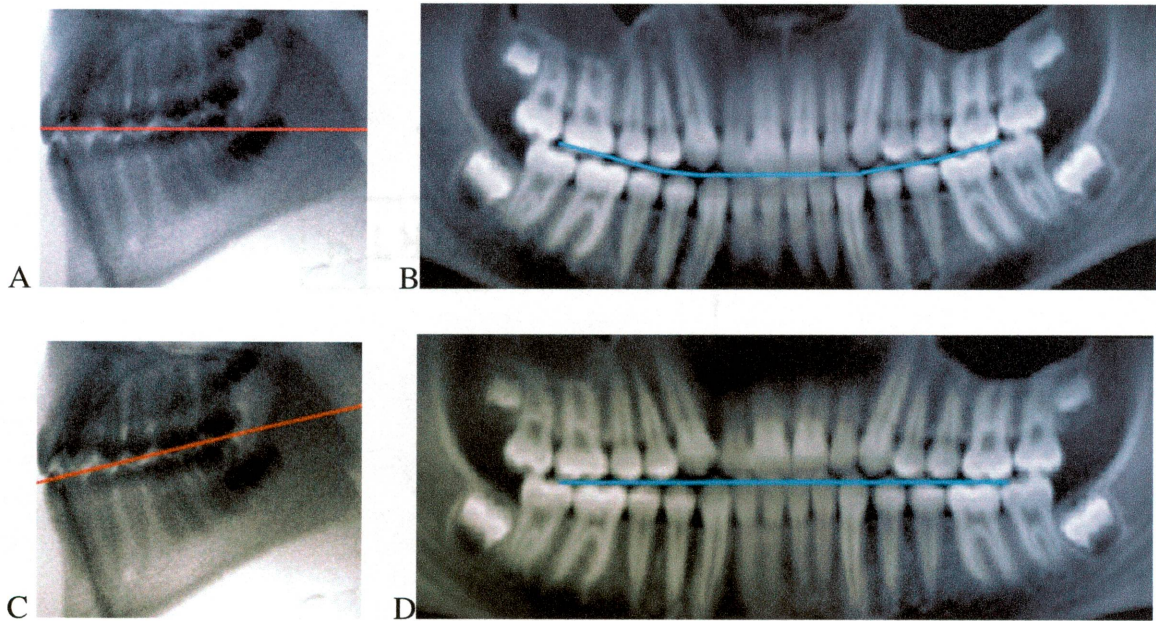
Fig. 28. Occlusal Plane Effect. (A) Functional occlusal plane not parallel to the red line. The image produced an obvious curve of Spee (B). (C) Functional occlusal plane reconstructed to parallel the red line. The image produced a flat occlusal plane (D).

Overall, the mean differences were higher on the right side than on the left side. There were several potential causes for these results. One factor may be the operator position during patient exposure. The patient may have had a tendency to slightly turn their head to the left side towards the voice of the operator. An illustration of this scenario using the phantom typodont is shown below (Fig. 29). Another potential factor could have been the lack of the calibration of temple calipers, the midline indicator, or motor synchronization.
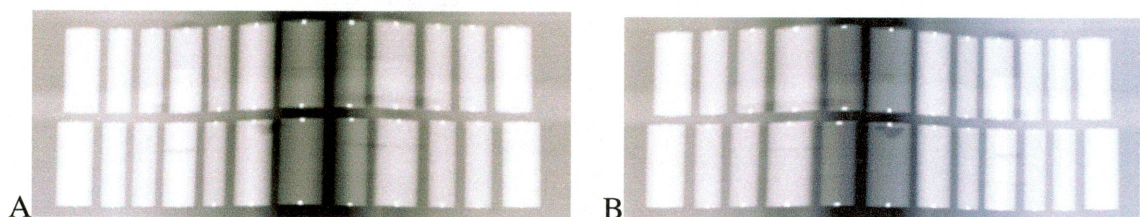
Fig. 29. Phantom Typodont Turn Effect. (A) Phantom typodont turned 15 degrees to the right creates magnification on the left side of the image. (B) Phantom typodont turned 15 degrees to left creates magnification on the right side of the image.

To confirm the increased magnification on the right side, 20 patients were selected randomly from the Sirona™ patient database and linear dimensions of the maxillary first molars were measured between the right and left side. Of the patients, 74% of the patients had magnification on the right side, 17% had magnification on the left side, and 9% were of equal magnification.

Archform Study

When comparing the mesial-distal width dimension of the first molars between the panoramic radiograph and each patient model, the value was greater for every panoramic radiograph, except one, which was of equal value. There was no statistical correlation between maxillary and mandibular width to the mesial-distal first molar dimensions for both the right and left side. Hypothetically, it is reasonable to assume that patients with wider jaws would have less magnification of the molar teeth due to the decreased object to film distance, and the opposite assumption would be true for patients with narrow jaws. In the panoramic unit, the temple support caliper device measured the patient skull and automatically selected a small, medium or large skull setting thus preventing any existing correlation. The trough size was selected to a particular dimension that would best fit the jaw size determined by the measured skull size. The assumption was that patients with larger skulls would have larger jaws. Because the panoramic unit automatically autofits the jaw to a focal trough based on the skull size, there should have been no correlation between the arch width and molar dimensional width.

Maxillary and mandibular depth of the right side showed no statistical correlation, but the left side did show a statistically significant correlation. For most panoramic units,

images become more magnified towards the posterior region of the arch. The question for this part of the study was to determine if patients with longer arch depth would have increased magnification in the posterior region, specifically the mesial-distal dimensions of the molar teeth. Again, the temple support calipers were used to move the patient's head forward or backward in order to comfortably position the patients incisors on the bite stick. The temple caliper position determined the start-stop radiation and again determined the focal trough selection. Results showed no correlation on the right side. The magnification on the right side of patient images may have precluded the existence of potential statistical significance. The left side corroborated the assumption that increased depth may magnify dimensional width. A possible explanation for the magnification on the right side of the patient images could have been due to patients slightly turning their heads toward the voice of the operator. The patient's midline would have been towards the left of the midline indicator line, and thus the position of the left molar would have been more posteriorly located than the right molar (Fig. 30).
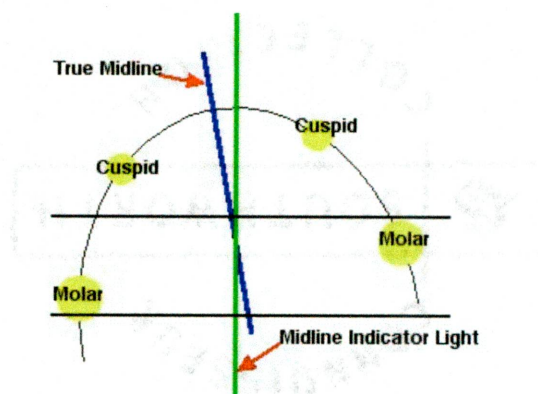
Fig. 30. Patient Head Turn Effect. As the patient's head is turned to the left, the left molar is positioned more posteriorly than the right molar.

For the linear dimensional accuracy study, the dimensional magnification discrepancies were all positive and were considerably high for the Sirona™ radiographs, when compared to their respective models. These results are consistent with current

literature findings on magnification distortion of panoramic radiographs. Although the dimensional magnification discrepancies between the Newtom 9000™ images to their respective models were much lower than the Sirona™, the overall results were higher than most current literature findings relating to dimensional accuracies of the Newtom 9000™. The magnification distortions were both positive and negative, which strongly points toward interpreter error. All measurements were made visually, hence inaccuracies could have been as a result of indistinguishable contact points due to factors such as interproximal overlap and image quality.

CHAPTER FIVE

CONCLUSIONS

The conclusions of this study are as follows:

1. In the typodont study, there were no angular differences between the Newtom 9000™ panoramic view and the Sirona™ panoramic radiograph.

2. In the patient study, the maxillary canine-premolar region showed the highest mean absolute difference between measurements acquired by the Newtom 9000™ panoramic images and the Sirona™ panoramic radiograph. The lowest difference was in the incisor and molar region. In the mandible, the highest mean absolute difference was in the posterior, and the lowest difference was in the anterior region.

3. In the archform study, there was no correlation between arch width and dimensional width of the first molars on the right and left side. For arch depth, there was no correlation on the right side, but there was a statistical correlation on the left side.

4. With the reconstructive capabilities of the Newtom 9000™, panoramic images using consistent methods that minimize image distortion can be obtained.

REFERENCES

1. Mayoral G. Treatment results with light wires studied by panoramic radiography. Am J Orthod. 1982 Jun; 81(6): 489-497.

2. Jarabak J, Fizzell J. Technique and treatment with light-wire edgewise appliances. The C.V. Mosby Company 1972; 2(7).

3. Ursi W, Almeida R, Tavano O, Henriques J. Assessment of mesiodistal axial inclination through panoramic radiography. J Clin Orthod 1990 Mar; 24(3): 166-173.Edwards J. The prevention of relapse in extraction cases. Am J Orthod 1971; 60:128-141.

4. Quintero J, Trosien A, Hatcher D, Kapila S. Craniofacial imaging in orthodontics: Historical perspective, current status, and future developments. Angle Orthodontist 1999; 69(6): 491-506.

5. Gomez-Roman G, Lukas D, Beniashvili R, Schulte W. Area-dependent enlargement ratios of panoramic tomography on orthograde patient positioning and its significance for implant dentistry. Int J Oral Maxillofac Implants 1999; 14(2): 248-256.Glass B, Seals R, Williams E. Common errors in panoramic radiography of edentulous patients. J Prosth 1994 June; 3(2): 68-73.

6. Langland O, Langlais, R, McDavid W, DelBalso A. Panoramic Radiology, 2nd Ed. Lea and Febiger Publishing. 1989.

7. Tronje G, Welander U, McDavid W, Morris C. Image distortions in rotational panoramic radiography Part I: General Considerations. Acta Radiologica Diagnosis 1981: 22:295-299.

8. Welander U. A mathematical model of narrow beam rotation methods. Acta Radio Diag 1974;15: 305.

9. McDavid W, Welander U, Brent Dove S, Tronje G. Digital imaging in rotational panoramic radiography. Dentomaxillofac Radiol 1995; 24(2): 68-75.

10. Tronje G, Eliasson S, Julin P, Welander U. Image distortion in rotational panoramic radiography Part II. Acta Radiologica Diagnosis 1981; 22(4): 449-455.

11. Wyatt D, Farman A, Orbell G, Silveira A, Scarfe W. Accuracy of dimensional and angular measurements from panoramic and lateral oblique radiographs. Dentomaxillofac Radiol 1995; 24(4): 225-331.

12. Hirschmann P. The current status of panoramic radiography 1987; 37:31-37.

13. Tronje G, Welander U, McDavid W, Morris C. Image distortions in rotational panoramic radiography Part III: Inclined Objects. Acta Radiologica Diagnosis 1981; 22(5): 585-592.

14. Lund T, Manson-Hing L. A study of the focal troughs of three panoramic dental x-ray machines: Part II. Oral Surg Oral Med Oral Pathol 1975 April; 39(4): 647-653.

15. Reiskin A. Implant Imaging: Status, Controversies, and New Developments. Dental Clin of North Amer 1998 Jan; 42(1): 47-55.

16. Mah J, Danforth R, Bumann A, Hatcher D. Radiation absorbed in maxillofacial imaging with a new digital computed tomography device.Oral Surg Oral Med Oral Pathol Oral Radiol Endod. 2003 Oct; 96(4): 508-513.

17. Glass B, Seals R, Williams E. Common errors in panoramic radiography of edentulous patients. J Prosth 1994 June; 3(2): 68-73.

18. McKee I, Williamson P, Lan E, Heo G, Glover K, Major P. The accuracy of four panoramic units in the projection of mesiodistal tooth angulations. Am J Orthod Dentofacial Orthop. 2002 Feb; 121(2): 166-175.

19. Philipp R, Hurst R. The cant of the occlusal plane and distortion in the panoramic radiograph. Angle Orthodontist 1978 Oct; 48(4): 317-323.

20. Lucchesi M, Wood R, Nortje C. Suitability of the panoramic radiograph for assessment of mesiodistal angulation of teeth in the buccal segments of the mandible. Am J orthod Dentofac Orthop 1988 Oct; 94(4): 303-310.

21. McKee I, Glover K, Williamson P, Lam E, Heo G, Major P. The Effect of Vertical and Horizontal Head Positioning in Panoramic Radiography on Mesiodistal Tooth Angulations. Angle Orthodontist 2001; 71: 442-451.

22. Samawi S, Burke P. Angular distortion in the orthopantomogram. Brit J Orthod 1984; 11: 100-107.

23. Edwards J. The prevention of relapse in extraction cases. Am J Orthod 1971; 60: 128-141.

24. Welander U, Tronje G, McDavid W. Layer thickness in rotational panoramic radiography: some specific aspects. Dentomaxillofac Radiol 1989 Aug; 18: 119-124.

25. Ziegler C, Woertche R, Brief J, Hassfeld S. Clinical indications for digital volume tomography in oral and maxillofacial surgery. Dentomaxillofac Radiol 2002; 31: 126-130.

26. Ludlow J, Davies-Ludlow L, Brooks S. Dosimetry of two extraoral direct digital imaging devices: Newtom 9000™ cone beam CT and Orthophos Plus DS panoramic unit. Dentomaxillofac Radiol. 2003 Jul; 32(4): 229-234.

27. Hatcher D, Aboudara C. Diagnosis goes digital. Am J Orthod Dentofac Orthop 2004 Apr; 125(4): 512-515.

28. Mozza P, Procacci C, Tacconi A, Tinazzi Martini P, Bergamo Andreis I. A new volumetric CT machine for dental imaging based on the cone-beam technique: preliminary results. European Radiology 1998; 8: 1158-1564.

29. Hsu, Shelton. The effect of mandibular distraction osteogenesis on condylar rotation in rabbits [Master's Thesis]. Graduate Orthodontic Program at Loma Linda University, 2002.

30. Moser, Noel. Linder-Aronson's analysis using rhinomanometry and Newtom 9000™ [Master's Thesis]. Graduate Orthodontic Program at Loma Linda University, 2002.

31. Rejebian G. A statistical correlation of individual tooth size distortions on the orthopantomographic radiograph. Am J Orthod 1979 May;75(5): 525-533.

APPENDIX Raw Data I

Phantom Study

KEY: d-degree X=Maxilla D=Mandible R=Right L=Left PA=Panoramic Radiograph NT=Newtom PH=Phantom
6=1st Molar 5=2nd Premolar 4=1st Premolar 3=Cuspid 2=Lateral 1=Central

SUB#	XR6.PA	XR6.NT	XR6.PH	XR5.PA	XR5.NT	XR5.PH	XR4.PA	XR4.NT	XR4.PH	XR3.PA	XR3.NT	XR3.PH	XR2.PA
#1- 0 d	0	0	0	0	0	0	0	0	0	0	0	0	0
#2- 0 d	0	0	0	0	0	0	0	0	0	1	0	0	1
#3- 0 d	0	0	0	0	0	0	0	0	0	0.5	0	0	0.5
#1- 10 d	10	11.1	10	10	10.6	10	10	10.7	10	10	10.7	10	10.5
#2- 10 d	10	10	10	10	10.2	10	10	10.6	10	10	10	10	10
#3- 10 d	10	10.9	10	10	10.7	10	10	10.5	10	10	10.5	10	10.5

SUB#	XR2.NT	XR2.PH	XR1.PA	XR1.NT	XR1.PH	XL1.PA	XL1.NT	XL1.PH	XL2.PA	XL2.NT	XL2.PH	XL3.PA	XL3.NT
#1- 0 d	0	0	0	0	0	0	0	0	0	0	0	0	0
#2- 0 d	0	0	0	0	0	0	0	0	0	0	0	0	0
#3- 0 d	0	0	0	0	0	0	0	0	0	0	0	0	0
#1- 10 d	10.4	10	10	10.7	10	11	11.1	10	10.5	11.4	10	0	10.8
#1- 10 d	10.7	10	10	11.2	10	11	9.6	10	10.5	9.9	10	10.5	9.9
#1- 10 d	9.3	10	11	10.1	10	12	9.3	10	10	9.9	10	10.5	9.8

SUB#	XL3.PH	XL4.PA	XL4.NT	XL4.PH	XL5.PA	XL5.NT	XL5.PH	XL6.PA	XL6.NT	XL6.PH	DR6.PA	DR6.NT	DR5.PA
#1- 0 d	0	0	0	0	0	0	0	0	0	0	0	0	0
#2- 0 d	0	0	0	0	0	0	0	0	0	0	0	-0.5	0
#3- 0 d	0	0	0	0	0	0	0	0	0	0	0	0	0
#1- 10 d	10	0	11.6	10	0	11.9	10	0	10.9	10	10.5	10	10.5
#2- 10 d	10	10.5	10	10	10.5	9.2	10	12	9.6	10	10	10.1	10
#3- 10 d	10	10	9.9	10	10	10.7	10	10.5	10.3	10	11	9.8	12

SUB#	DR5.NT	DR5.PH	DR4.PA	DR4.NT	DR4.PH	DR3.PA	DR3.NT	DR3.PH	DR2.PA	DR2.NT	DR2.PH	DR1.PA	DR1.NT
#1- 0 d	0	0	0	0	0	0	0	0	0	0	0	0	0
#2- 0 d	0	0	0	0	0	-0.5	0	0	0	0	0	0	0
#3- 0 d	0	0	0	0	0	0	0	0	0	0	0	0	0
#1- 10 d	9.8	10	10.5	10	10	10	10.5	10	10.5	9.1	10	10	10.8
#2- 10 d	10	10	10	9.9	10	10	10.2	10	10	10.2	10	10	10.4
#2- 10 d	9.2	10	12	10	10	12	10.8	10	12	10	10	14	9.4

SUB#	DR1.PH	DL1.PA	DL1.NT	DL1.PH	DL2.PA	DL2.NT	DL2.PH	DL3.PA	DL3.NT	DL3.PH	DL4.PA	DL4.NT	DL4.PH
#1- 0 d	0	0	0	0	0.5	0	0	0.5	0	0	0	0	0
#2- 0 d	0	0	0	0	0	0	0	0	0	0	0	0	0
#3- 0 d	0	0	0	0	0	0	0	0	0	0	0	0	0
#1- 10 d	10	10.5	9.9	10	10	10.1	10	10	9.1	10	9.5	9.6	10
#2- 10 d	10	10.5	9.9	10	10	11.1	10	10	10.7	10	9.5	12	10
#3- 10 d	10	12.5	11.2	10	10	10.9	10	10	10.2	10	10	10.6	10

SUB#	DL5.PA	DL5.NT	DL5.PH	DL6.PA	DL6.NT	DL6.PH
#1- 0 d	0	0	0	0	0	0
#2- 0 d	-1	0	0	-0.5	0	0
#3- 0 d	0	0	0	0	0	0
#1- 10 d	9.5	10.1	10	10	9.2	10
#2- 10 d	9.5	11.6	10	9.5	10.5	10
#3- 10 d	10	9.7	10	10	9.9	10

Appendix II Raw Data
Mean Absolute Angular Difference Between the Newtom and the Sirona

KEY: X=Maxilla D=Mandible R=Right L=Left P=Panoramic Radiograph N=Newtom
1= Central   2=Lateral   3=Cuspid   4=1st Premolar   5=2nd Premolar   6=1st Molar

Sub#	XR6.P	XR6.N	XR5.P	XR5.N	XR4.P	XR4.N	XR3.P	XR3.N	XR2.P	XR2.N	XR1.P	XR1.N	XL1.P	XL1.N
1	0	10.9	-5	11.7	0	11.7	-1	14.5	-7	8.9	-2	-4	1.5	2.2
2	1.5	10.3	-1	5.7	1	14.5	1	20.6	-7	4.1	2	17.2	-1	5.7
3	-4	0	-2	6.7	-1	9.3	-2	17.8	-3	13.6	-3	2.4	4	7.8
4	5	12.9	0	12.9	-1	14.5	-3	15.4	-8	16.7	-3	9	1	18
5	-2	13.2	-8	10.8	-8	14.7	-5	17.3	-5	14	-2	18.7	-2	11.7
6	5	10.6	0	7.5	0	9.6	1	10.9	0	3.4	0	4.7	1	6.8
7	3	0	-3.5	1.1			3	13.5	-6	0	0	5.6	1	1.1
8	12	15.8	1	13.2	4.5	12.8	2.5	16.4	-2	0	-1.5	1.9	0	0
9	8	19.7	1	11.9			0	20.1	0	-5.3	5	3.3	2	7.5
10	0	7.5	-8	5.7	-3	4.6	4	20.3	-7	4.8	8	16.3	-2	11.7
11	9	9.3	-10	4.3			0	19.3	-2	2.9	-1	3.1	4	7.8
12	9	12.7	-5	8.7	-8	7.3	-5	16.3	-7	11.3	-4	15.6	3	8.3
13	9	10.6	-10	1.1	-5	5.6	-5	6.5	-5	-3.6	-3	0	2	0
14	5	10.2	-7	0	-2	11.1	-2	11.3	-6	-3.4	-4	-4.5	8	7.1
15	-9	-1.3	-14	3.4			-3	17.8	-5	4.8	-2	5.7	2	2.5
16	-1	6.1	-4	8.1	-2	13.3	-1	11.9	-1	13.5	-1	11.3	0	7.4
17	3	3.6					0	19	-4	-2.4	-7	0	2	2.2
18	3	8	0	15.5	1	22.4	0	21.1	-2	7.3	0	7.7	0	0
19	4	2.6	-5	0	-5	4	0	8.5	-3	6.6	0	5.1	0	5.9
20	2	0	-5	0			-5	10.3	-8	0	-6	0	-1	-6.2
21	1	0	-5	0	0	3.7	-3	8.7	-3	0	1	1.2	5	9.5
22	5	10.9	1	12.5	7	22	5	26	-2	8.7	-3	0	3	2.9
23	1	2.5	-7	0	-2	5.8	-3	10.9	-5	3.4	-7	0	3	3.7
24	5	4.8	1	0	-2	3.6	4	7.7	-6	0	5	5.6	0	3.6
25	-3	1.8	-7	-5.3	0	7.7	0	9	-2	2	0	4.2	1	3.2
26	10	10	0	8	0	8.9	-1	7.4	-3	4.6	2	5.7	5	7.4
27	12	5.8	0	5			-1	9.9	0	7.3	0	4.7	1	2.6
28	4	8.2	-8	0			-4	7	-6	6.5	-3	4.5	5	2.3
29	12	4.7	0	3.7	1	5.2	3	12.8	1	9.1	1	5.3	2	4
30	2	0	-7	2.3	-9	7.3	-3	5.6	-11	2.4	-2	7	-4	5.8
31	5	7.3	-3	3.5	-5	9.7	9	24.7	-7	0	0	12.8	5	11.6
32	2	9	0	7.4	-7	0	2	15.9	0	9.6	11	19.3	-1	7
33	6	9.9	1	10.5	-2	12.1	0	11.6	-9	0	-4	0	3	0
34	15	11.8	2	12.1			6.5	18.7			1	5.4	2.5	8.8
35	8	-2	-1	2.3	5	11.3	0	5.9	-2	5.9	0	7.3	2	9.7
36	-10	-1.2	-19	-5.2	-12	0	-9	11.7	-16	2.2	0	3.3	0	1.1
37	3	-1.2					-7	3.8	-9	-5.7	-2	4.2	1	0
38	-1	-7.7	-5	0			-2	12.8	-12	-8.5	0	6.6	1	4.8
39	7	4.7	1	5.5	1	8.1	-5	9.5	-9	0	-3	0	-1	4.9
40	2	0					-1	17.4	-16	5.8	-8	-3.7	8	11.3
41	8	6.8	11	5.7			1	13.3	-1	4.1	-3	4.6	5	6.8
42	2	6.5	-11	1.4	-6	6.3	-1	13.7	-6	5.6	-2	7	2	3.6
43	11	9.1	2	4.9	12	12.4			1	8.4	2	14.8	7	9.1
44	6	12.6	-9	7.1	-7	9.6	0	14.9	-3	0	-2	0	2	0
45	-1	7.3	-18	-3.5	-9	8.7	-5	11.1	-11	3.4	-6	7.8	0	4.8
46	2	6.6					0	0	-8	-3.9	-2	0	7	8.7
47	-18	7.2	-13	8.1			-1	21.3	-6	15.2	-3	6.1	3	6.2
48	-2	4.9	-14	3.6	-6	5.8	-11	8.4	-6	2.2	-2	6.2	6	7.3
49	4	10	-3	9.5	-1	9.6	-6	10.7	-6	0	-2	4.5	0	4.6
50	7	2.7	0	2.5	2	5.8	3	11.7	-3	7.4	-2	13.5	3	8.1
51	-2	-4.2	-10	0	-2	6.8	0	27	-15	-7.9	-3	6.1	6	3.5
52	-2	-4.3	-9	0			-2	15.3	-6	3.5	5	12.4	7	14.7
53	12	5.5					-2	19.1	-5	3.9	4	9.5	1	14.2
54	8	8.4					-2	14.4	-2	-2.4	2	2.3	3	6.1
55	3	0	-1	0	-2	6.1	7	6.8	-5	0	5	9.3	8	5.9
56	-15	11	-20	13.7	-6	4.5	-13	2.3	-18	1.1	-8	7.8	-6	7.6
57	-11	-9			-3	12.3	0	13.8	-6	0	-4	1.1	4	1
58	0	3.5	-3	0	1	3.5	5	11.1						
59	-8	0	0	10.4			10	17.2			0	0	0	0
60	6	5.3	-12	0	0	6.3			-6	3.6	0	5	8	4.2

Appendix II Raw Data
Mean Absolute Angular Difference Between the Newtom and the Sirona

KEY: X=Maxilla D=Mandible R=Right L=Left P=Panoramic Radiograph N=Newtom
1= Central   2=Lateral   3=Cuspid   4=1st Premolar   5=2nd Premolar   6=1st Molar

Sub#	XL2.P	XL2.N	XL3.P	XL3.N	XL4.P	XL4.N	XL5.P	XL5.N	XL6.P	XL6.N	DR6.P	DR6.N	DR5.P	DR5.N
1	-2	3.2	-1	16.4	2	13.7	-2	8.1	2	7.3	26	9.5	20	6.7
2	-8	3.3	0	18.4	0	8	-1.5	5.7	6	10.6	28	15.5	15	5.9
3	0	11.3	0	20.2	-2	11.5	-2	8.3	-2	2.2	20	8.4	5	3.3
4	-4	21.5	-2	21.3	0	17.5	-6	3	3	14.8	25	10.5	24	5.8
5	-9	7	-4	19.6	-4	18.4	-6	10.5	-5	8.5	38	13.3	18	1.2
6	2	4.9	0	6.7	0	9.6	-4	5.7	2.5	9	25	5.1	16	6.8
7	-2.5	-2.5	2.5	12.5			-7	1.1	2	3	21	11.6	15	6.7
8	0	-4.9	1	10.7	2	12	5	8.7	11	15.6	18	10.9	12	5.4
9	-3	3.2	0	11.3			-3	7.4	7	18.4	28	10.5	15	7.6
10	-12	7.7	5	19.9			-6	5.7	2	5	26	7.9	15	8.7
11	2	6.8	0	6.7			-8	-2	6	8.6	26	15.9	18	9.6
12	0	5.1	1	10.2	-5	7.7	-2	7.6	-2	3.5	22	12.4	15	3.4
13	0	-3.8	-1	13.5	0	7.3	-2	1.1	11	12.5	24	14.7	14	9.1
14	-2	0	4	12.2	3	10	0	0	7	8.4	30	19	17	12.7
15	-4	0	4	27			-4	6.8	32	2.8	26	15.9	18	3.1
16	-6	6.7	-5	7.7	-4	5.4	-7	4.5	4	7.8	23	10.6	14	2.7
17	-3	-7.7	2	13.8					3	3.6	25	14.2	17	10.5
18	3	0	6	17.8	5	15.1	3	6.6	7	7.3	32	16.3	23	10.4
19	0	3	0	9.2	0	4.5	-5	0	4	0	21	14.7	15	9.7
20	-6	-13.2	-1	8.6			0	-7.7	3	3.5	22	16.8	21	4.4
21	2	4.3	0	2.4	-1	-4.7	-1	-2.7	3	2.9	16	11.6	8	7.5
22	0	13	7	21.5	5	18.1	4	14	7	11.4	21	12.3	16	5.9
23	-1	0	0	5	-3	2.6	-6	-11.8	4	3.3	16	12.7	14	12.1
24	-4	0	1	3.8			-3	-4.7	7	2.1	30	22.3	19	14.6
25	-5	0	0	8	1	3.6	-8	6.7	-2	2.6	31	26.6	11	7.7
26	0	0	1	10.7	6	11.9	5	11.1	7	11.3	28	22.3	17	14.6
27	1	5.8	1	8			4	0	13	5.8	15	15.3	7	9.3
28	-2	0	0	7.1			-2	4.6	6	5.1	35	19.8	25	12.1
29	0	0	12	18	10	19.4	8	8.4	14	10.1	20	19.5	5	5
30	-8	0	-4	4.9	-4	5.8	-11	0	0	2.3	28	13.8	20	9.5
31	2	3.7	8	24	3	9.1	1	5.7	7	6.4	25	13.7	10	6.2
32	0	7.6	12	15.3	-2	7.6	1	6.3	6	7.2	22	13.3	13	6.2
33	0	0	3	13	2	13.3	1	6.3	2	1.5	27	20.6	18	15.4
34			3.5	14			-2.5	3.3	3	8	27	16	18	13.2
35	1	4.1	-1	6			-2	0	7	-1.4	26	21.7	19	18.4
36	-11	-4.1	-8	0			-19	-8.1	-10	2	35	20.7	28	12.9
37	-8	-5.9	-5	0					-4	7	29	19.7	17	8.5
38	-6	-6.3	0	6.8			-4	0	0	2.6	34	21.9	22	10.7
39	-6	0	1	5.7	2	2.5	-4	0	7	4	26	17.7	13	13.1
40	-4	2.5	10	14.6					8	4.7	19	17.2	5	6.3
41	2	4.5	2	14.5	2	7.7	1	5.6	7	4.4	30	16.2	18	8.9
42	-10	3.8	-4	7			-7	0	2	7	26	18.7	19	8
43	2	10.4	9	14	14	14.3	2	6.5	16	9.8	25	15	2	-1.2
44	0	2.4	3	14.8	-1	9.3	-3	4.9	7	11.1	21	9.2	9	0
45	-10	0	-12	-3.6	-8	2.9	-9	-2.5	-4	5.2	30	15.1	26	9.6
46	2	0	9	14	4	0	2	1.6	3	6.7	8	9.5	2	6.5
47	2	11.1	10	34.3			-1	12.1	-4	9	30	9	19	0
48	0	10.7	0	11.1	2	11.8	-10	4.2	-5	0	30	17.5	18	12.2
49	-1	6.7	-1	9.6	-2	10.8	-5	6.8	2	4.2	19	6	9	-1.3
50	0	0	8	15.3	8	9.7	4	6.6	7	4.2	14	9.2		
51	0	0	6	12	-7	5.2	-8	-2.5	-5	-4	21	11.5	14	8.7
52	-2	3.2	1	7.3			-1	-1.3	-4	-3.3	25	19.2	10	9.3
53	-8	8.1	-3	20.6					9	11.6	24	14	12	4.3
54	2	0	2	7.6			10	13.8	12	10.4	25	19.5	9	8.7
55	7	6.2	7	8	7	5.9	5	2.7	7	1.9	15	13.7	12	13.3
56	-9	0	-8	-2.9	0	11.3	-10	12.9	-9	7.3	36	25.8	25	10.3
57	-4	0	0	5.4	-5	3.8			-9	6.9	26	20.8	15	6.1
58			7	5.8			1	0	8	5.2	17	11.8	13	3.8
59	-2	3.4	-3	15	2	12.7	2	10.3	0	7.6	25	8.9	18	5.7
60	6	7.8	4	3.6	-7	2.6	-14	-9.8	9	7.3	27	14.5	18	12.2

Mean Absolute Angular Difference Between the Newtom and the Sirona

KEY: X=Maxilla D=Mandible R=Right L=Left P=Panoramic Radiograph N=Newtom
1= Central   2=Lateral   3=Cuspid   4=1st Premolar   5=2nd Premolar   6=1st Molar

Sub#	DR4.P	DR4.N	DR3.P	DR3.N	DR2.P	DR2.N	DR1.P	DR1.N	DL1.P	DL1.N	DL2.P	DL2.N	DL3.P	DL3.N
1	12	2.3	5	-4.3	0	3.2	5	0	-2	0	-3	0	-1.5	0
2	9	5.4	5	2.2	-3	5.3	-1	1.5	4.5	1.1	5	2.5	3	
3	7	2.2	2	3.8	6.5	6.5	2	9.2	4	1.2	10	1.5	8	1.5
4	20	6.8	16	9.1	5	5.8	0	10.4	1	-7.1	0	-3.9	10	3.6
5	14	0	19	5	0	2.7	0	2.9	-1	-3.2	3	0	12	7.1
6	13	9.1	13	9	10	7.1	0	8.7	5	3	6	2.8	17	3
7	7	3	7	3.1	5	-2.4	5	3.2	-2.5	-4.2	-3	-2.2	2	0
8	13	7	-6	3.9	-2	3.1	-2	0	1	0	0	0	-1	0
9	17	12.2	13	10.5	3	7.8	2	3	4	0	6	1.2	13	2.4
10	4	2.3	6	8	-4	-2.2	-3	3.7	0	0	0	-1.2	9	8.6
11	13	11.8	5	0	4	3.8	3	5.6	-1	-2.4	0	-2.7	-3	-15.6
12	9	3.6	8	5.7	4	4	2	0	5	5.7	7	3.7	10	5
13	6	4.9	0	4.9	1	4.4	-2	0	-4	-2.8	-5	-3	-2	2.6
14	5	0	1	3.9	-1	3.6	0	4.7	2	-3.7	9	12.8	10	4.9
15	10	0	8	0	-2	0	0	0	2	0	-1	-3.2	3	0
16	3	-4.5	4	1.5	-4	-9.9	1	-4.1	-2	0	-4	0	-5	-3.7
17	13	5.9	7	7.9	-1	0	0	0	0	0	-3	-8.8	1	-3.8
18	13	8.1	7	4.6	3	0	3	0	1	7.9	3	5.7	2	5.1
19	2	4.7	1	-3.4	2	1.4	2	4.8	-2	5.4	-6	0	-3	2
20	9	4.4	3	4.1	0	0	-1	0	0	5.2	-1	5.9	-4	9.2
21	4	5.2	3	3.5	-2	3.8	-1	10.2	3	5.4	2	4.9	4	5.3
22	11	4.8	8	7.4	7	5.8	-2	0	1	7.1	4	11.3	7	9.5
23	8	11.6	-9	0	-11	-3.1	-11	0	10	6.7	3	0	2	2.9
24	15	12.8	15	16.1	4	0	3	0	4	0	4	4.4	9	7.9
25	1	0	5	6.9	-1	0	0	0	0	0	-2	3.4	0	3.7
26	9	7.3	8	4.5	0	0	2	0	-2	0	-5	5.6	5	6.5
27	0	4.2	-6	0	-6	9.2	-1	0	6	6.4	0	4.9	-5	5.6
28	2	-12.2	3	-3.3	-1	-4.7	-1	-2.9	4	7.8	-2	-3.2	-2	-3.4
29	1	4.3	3	8	-4	-2.4	0	0	-2	0	-3	5	-6	3.1
30	8	6.8	-1	2.5	-6	0	-6	0	2	0	-1	0	4	6.3
31	9	8.8	10	7.4	0	-4.4	2	-3.5	-2	0	-11	3.3	-1	5.1
32	10	10.9	7	13.2	-3	8.5	4	7	-2	1.3	-6	2.3	8	10.5
33	13	12.8	8	16.3	5	11.8	-5	4	6	0	5	0	8	6.8
34	13	12.5	5	13.1	-7	1.2	-9	0	9	1.2	4	0	17	15.3
35	8	18.8	7	18.7	-1	3.7	-2	4	-2	4.2	1	0	1	14.6
36	20	6.6	17	7.7	-2	-5.4	0	0	0	6.8	2	2.6	13	7.3
37	6	3.2	1	6.8	-2	2	-3	-6.7	0	1.5	0	8.8	1	8.7
38	13	8.1	4	2.1	1	2.1	1	0	0	0	-1	0	7	7.1
39	7	9.5	-2	9.9	-4	6.1	-1	4.8	0	0	1	5.3	5	8.1
40	3	9.9	0	8.4	-10	-2.9	-6	5.7	-1	-7.5	-5	-6	2	2.7
41	10	8.8	5	16.8	1	7.1	-3	1.4	3	0	13	2.9	8	8.6
42	19	9.5	13	9.6	2	0	6	0	0	8.1	1	11.9	19	13.7
43	4	1.2	0	10.2	-6	1.4	-5	0	7	3.1	6	1.5	5	2.6
44	9	0	5	-2.5	1	-6.3	1	-2.7	0	1.5	-3	-4.8	2	-2.5
45	11	1.2	1	-3.1	-6	-1.3	-5	0	5	0	5	0	11	6.5
46	0	6.7	-2	8.1	-7	8.3	-5	7.5	10	-5.8	6	1	1	4.2
47	16	7.8	17	7.5	4	-2.3	1	-4.9	0	4.8	6	4.8	15	8.5
48	9	8.7	10	11.3	1	-4	2	5.9	9	5.4	2	-1.2	5	0
49	9	2.7	6	3	1	0	2	0	2	-1.9	-12	-12.8	2	1.6
50	5	2.4	9	7.3	5	4	5	4.2	-3	2.8	-4	2.7	3	4.2
51	11	9.1	-1	3.4	-10	-3.8	-7	0	3	0	-1	-12.4	0	-10
52	-5	-4.8	-11	1.7	-12	0	-9	0	5	0	0	-1.2	0	-2.5
53	9	3.4	0	4	-1	0	0	0	3	0	3	0	3	0
54	0	0	-5	2.3	-6	-5.9	-2	0	1	0	-5	0	-3	0
55	7	10	4	11.1	-7	0	-5	5.9	-5	10.3	-2	0.9	1	7
56	8	5.6	11	10	3	8.7	0	9	0	2.2	-1	4.7	8	2.5
57	3	0	5	7.3	5	6.1	7	3.7	0	2.9	0	4.1	0	8.9
58	6	1.8	3	0	-7	3.5	-3	0	2	0	-2	0	-3	4.5
59	1	-5.1	-10	-7.9	-8	0	-5	2.9	3	1.5	2	3.4	2	0
60	20	14.6	10	8.5	4	6.2	4	-5.7	3	4	5	6.2	1	2.5

Mean Absolute Angular Difference Between the Newtom and the Sirona

KEY: X=Maxilla D=Mandible R=Right L=Left P=Panoramic Radiograph N=Newtom
1= Central 2=Lateral 3=Cuspid 4=1st Premolar 5=2nd Premolar 6=1st Molar

Sub#	DL4.P	DL4.N	DL5.P	DL5.N	DL6.P	DL6.N
1	8	2.8	13	4.4	26	11.9
2	7.5	1.4	11	1.4	25	13.8
3	8	1.3	11	1.2	19	6.1
4	16	3.6	18	2.9	25	8.8
5	19	7.8	20	2.2	28	11.6
6	8	-2.8	12	1.8	24	9.6
7	4	0	12	5.9	20	9.1
8	8.5	5.9	13	4.4	17	11.3
9	11	5	14	2.5	23	5.9
10	8	0	19	6.1	25	11.9
11	9	6.5	12	3.4	31	15.2
12	10	3.5	15	6.1	22	14.9
13	5	4	11	9.7	25	14.4
14	9	3.4	15	12.9	31	21.4
15	8	0	19	6	32	15.7
16	4	0	18	6.7	23	8.6
17	5	0	12	5.4	23	12.9
18	12	4.9	26	13.4	26	17.3
19	2	2.9	18	12.8	28	16.9
20	-7	6.2	5	6.1	24	19.3
21	1	2.3	9	5.2	19	9.6
22	6	0	17	10.8	21	11.6
23	6	10.8	14	12.4	22	16.3
24	8	0			28	16.3
25	0	0	11	7.8	33	25.6
26	8	8.4	14	10.2	30	20.5
27	-4	3.8	2	8.7	19	17.6
28	0	-10.8	2	0	27	19.3
29	-3	3.5	-1	5.6	17	16.2
30	8	5.9	26	15.7	29	17.9
31	-2	8.5	9	7.3	25	11.4
32	11	7.7	8	4.9	23	13.3
33	10	7	20	12.2	27	20.7
34	17	10.6	26	14.6	30	22.8
35	11	11.3	14	13.7	30	25.7
36	16	7.8	24	10.3	35	19.3
37	2	3.3	11	8.4	31	24.8
38	15	13.1	34	24.2	25	11.4
39	4	8.5	10	13.6	21	14.6
40	2	0	1	3	17	14.8
41	7	3.7	17	9.6	22	14.7
42	16	11.9	21	13.3	28	20.2
43	3	0	3	0	13	15.4
44	2	-7.9	8	-2.7	24	9.1
45	15	2.2	27	12.7	38	20.9
46	1	2.1	4	6.9	8	8.1
47	15	5.7	20	8.3	32	16.6
48	13	12.5	23	11.5	27	14.7
49	2	-1.7	13	1.6	22	8.2
50	-1	0	8	3.7	15	10.2
51	11	12.1	12	5.3	24	10.2
52	-5	-2.6	10	5.2	25	21.4
53	8	0	9	0	17	10.7
54	0	2.5	6	4.4	27	20.2
55	3	9.5	10	11	15	14
56	12	8.7	22	9.8	34	20.9
57	-1	4.3	15	11.8	29	20.7
58	-3	1.5	7	7.7	17	14
59	2	-4	15	5.9	20	10.2
60	7	6.2	15	11	25	15.7

APPENDIX III Raw Data

Patient Angle Rechecked Values

KEY: X=Maxilla D=Mandible R=Right L=Left P=Panoramic Radiograph N=Newtom
1=Central 2=Lateral 3=Cuspid 4=1st Premolar 5=2nd Premolar 6=1st Molar

sub.#	XR6P1	XR6P2	XR6P3	XR6N1	XR6N2	XR6N3	XL3P1	XL3P2	XL3P3	XL3N1	XL3N2	XL3N3
1	0	0	0	10.9	11.7	9.8	-1	0	-1	16.6	15.5	16.4
4	5	4	4	12.9	13	13.8	-2	0	0	21.3	21.3	20.9
7	2	3	3	0	0	0	2.5	2	2	14	13.5	12.5
10	0	1	1	7.5	8	8.1	3	4	5	18	19.9	21
13	7	9	9	10.6	10.5	10.9	0	1	1	13.5	15.9	16.3
16	-1	-3	-2	6.1	6.6	6.9	-5	-5	-5	7.7	8.5	8.3
19	4	4	4	2.6	2.4	4.6	1	2	3	9.2	8.1	8.9
22	5	4	6	10.9	11.9	10.8	8	6	7	21.5	22.9	23
25	-3	-3	-4	1.8	1.8	3.1	0	0	0	8	9.5	9.9
28	4	5	5	8.2	8.5	6.3	0	0	0	6.5	7.1	7.5
31	5	6	5	7.3	7.3	8.1	8	8	8	24	24.5	24.8
34	15	14	13	11.8	11.9	12.2	3.5	4	4	14.4	13.8	14
37	3	2	2	-1.2	-0.8	-2	-5	-6	-5	0	0	0
40	2	3	3	0	0	0	11	12	13	14.6	16.2	16
43	11	13	11	7.7	9.1	9.1	9	10	9	14	14.6	14
46	2	2	2	6.6	6	6.6	7	8	9	14.5	13.8	14
49	5	3	4	10	9.3	9.6	-1	-1	-1	9.6	10	11.7
52	-1	-2	-2	-3.7	-4.3	-5.5	1	2	2	6.7	7.3	7.4
55	4	4	3	0	0	0	7	8	8	8	7.2	8.6
58	1	0	0	3.5	2.1	3.9	11	13	12	5.8	5.6	4.7

APPENDIX III Raw Data

Patient Angle Rechecked Values

KEY: X=Maxilla D=Mandible R=Right L=Left P=Panoramic Radiograph N=Newtom
1=Central 2=Lateral 3=Cuspid 4=1st Premolar 5=2nd Premolar 6=1st Molar

sub.#	DR4P1	DR4P2	DR4P3	DR4N1	DR4N2	DR4N3	DL2P1	DL2P2	DL2P3	DL2N1	DL2N2	DL2N3
1	12	13	13	2.9	2.3	4.3	-3	-4	-4	3.2	2.9	3.9
4	20	20	20	6.8	7.5	8.9	0	0	0	3.9	5.8	5.4
7	7	8	9	3	2.8	3.4	-3	-3	-3	-2.2	-2.4	-1.9
10	4	3	3	2.3	3.6	2.5	0	1	1	-3.4	-1.2	-2.3
13	6	4	6	6.3	4.8	4.9	-5	-6	-6	3	3.4	2.2
16	3	3	4	4.5	3.6	4.8	-4	-4	-3	0	0	1.9
19	2	2	2	4.9	4.7	5.8	-6	-8	-8	0	0	0
22	11	10	10	4.7	4.8	4.5	4	4	5	9.3	9.3	11.3
25	1	0	0	0	0	0	-2	-3	-3	3.4	2.6	2.4
28	3	4	4	13.8	12.2	13.6	-2	-4	-4	-3.2	-3.6	-3.4
31	9	10	10	8.8	9	10.1	-11	-13	-13	4.5	3.3	4.1
34	13	11	11	12.7	12.5	14	4	5	4	0	0	0
37	6	6	7	2.4	2.5	3.2	0	0	0	10.5	8.8	9.3
40	3	0	0	9.9	8.8	7.9	2	2	3	6	6.8	7.1
43	2	0	0	0	0	1.2	6	7	6	1.5	1.5	1.4
46	-2	-2	-2	5.3	5.2	6.7	6	6	5	1	2.9	2.6
49	9	9	9	3.8	4.6	2.7	-12	-14	-14	12.8	13.8	14
52	-5	-6	-6	-4.8	-4	-4.1	0	0	0	-1.2	-0.9	-0.9
55	7	7	7	10	11.6	10.6	-2	-2	-2	2.3	0.9	2.3
58	6	7	6	1.8	1.6	1.3	-2	-2	-2	0	0	0

Appendix IV Raw Data

Archform Study

KEY: X=Maxilla D=Mandible W=Width D=Depth R=Right L=Left M=Model
P=Panoramic Radiograph 6=1st Molar d=Difference N=Newtom

Pt.#	XW	XD	XR 6-M	XR 6-P	d	XL 6-M	XL 6-P	d	DW	DL	DR 6-M	DR 6-P	d	DL 6-M	DL 6-P	d	DR 6-N	DL 6-N
1	41	26	10.5	13.1	2.6	10.5	11.8	1.3	33	21	10.5	13.2	2.7	10.5	11.6	1.1	10.4	10.4
2	41	32	11	13.4	2.4	11	12.5	1.5	40	26	11	13.7	2.7	11	13.1	2.1	11.3	11.3
3	41	31	10	12.1	2.1	10	12.9	2.9	39	23	10.5	13.7	3.2	10	13.5	3.5	11	11
4	45	29	10	11.9	1.9	10	10.9	0.9	43	22	10.5	11.6	1.1	10.5	11.7	1.2	10.7	10.7
5	47	28	11	13	2	11	11.7	0.7	42	22	11	13.7	2.7	11	13.4	2.4	11	11.3
6	45	24	10	11.5	1.5	10	11	1	40	20	11	12.7	1.7	11	11.3	0.3	10.7	11
7	45	27	11	13	2	11	13	2	39	28	11	13.8	2.8	11	13.7	2.7	11.3	11.6
8	43	26	10	12.9	2.9	10	11.3	1.3	42	18	11	13	2	11	11.4	0.4	11	11
9	43	21	11	13	2	11	12.4	1.4	38	22	11.5	14.2	2.7	11.5	14	2.5	11.3	11.9
10	44	27	11	12.7	1.7	11	13.6	2.6	40	22	11	12.7	1.7	11	14.5	3.5	11.3	11.3
11	41	25	10	12.3	2.3	10	11.7	1.7	39	20	10	13.4	3.4	10	11.4	1.4	10.5	10.5
12	45	28	11	13.5	2.5	11	12.5	1.5	40	24	12	15.6	3.6	12	14.2	2.2	12.2	12.2
13	39	25	9.5	11.9	2.4	10	10.2	0.2	36	20	10	13.3	3.3	10	10.8	0.8	10.5	10
14	43	22	10	11.9	1.9	10	11.2	1.2	40	22	9.5	11.5	2	9.5	10.8	1.3	10.3	10.2
15	50	31	12	12.5	0.5	11.5	12.3	0.8	43	28	11.5	14	2.5	11.5	14.1	2.6	11.9	11.6
16	42	29	10.5	13	2.5	10.5	11.5	1	37	25	11	13.7	2.7	11.5	13	1.5	11	11.3
17	42	25	10	10	0	10	11	1	38	28	10.5	11.5	2	9.5	12	2.5	10.5	10
18	46	30	11	12.7	1.7	11.5	13.5	2	43	25	11	14.5	3.5	12	14.2	2.2	12	11.9
19	46	27	12	13.4	1.4	11.5	13.1	1.6	40	21	12	14.5	2.5	12	14.9	2.9	12.3	12.5
20	48	29	10.5	11.5	1	10.5	11.2	0.7	43	29	10.5	12.2	1.7	10.5	12.2	1.7	10.5	10.5
21	43	27	10	12.7	2.7	10	11.7	1.7	36	22	9.5	13.2	3.7	9.5	12.5	3 x		x	
22	49	29	11.5	14.8	3.3	11.5	13.9	2.4	43	30	12	15.1	3.1	12	15.9	3.9	12.2	12
23	38	19	11	12.1	1.1	12	12.5	0.5	36	21	11	14.5	3.5	10.5	12.3	1.8	11	10.5
24	47	39	11	13	2	11	12.8	1.8	40	28	11.5	14.5	3	12	14.5	2.5	11.9	11.8
25	45	28	10	12.4	2.4	10	11.8	1.8	38	22	10.5	13.3	2.8	10.5	13.4	2.9	10.5	10.8
26	43	26	10	10.8	0.8	10	10.8	0.8	38	23	10	11.9	1.9	10	11.8	1.8 x		x	
27	38	26	10	11.9	1.9	10	11.4	1.4	35	22	10	12.1	2.1	10	12.3	2.3 x		x	
28	42	28	11	13.7	2.7	11	12.4	1.4	38	22	11.5	14.4	2.9	11.5	13.1	1.6	11.5	11.3
29	40	27	10	11.8	1.8	10	11.7	1.7	37	21	11	13.1	2.1	10.5	14	3.5	11.2	11.2
30	41	29	10.5	14.4	3.9	10	11.7	1.7	39	22	10	14.5	4.5	10	11.6	1.6 x		x	
31	40	27	11.5	13.6	2.1	11.5	12.4	0.9	34	21	11.5	13.9	2.4	11.5	13.2	1.7	11.3	11.3
32	43	27	10.5	12.2	1.7	10.5	12.5	2	40	22	10	12.5	2.5	10	12.5	2.5 x		x	
33	50	29	9.5	12.2	2.7	9.5	11.7	2.2	45	25	10.5	13.2	2.7	10.5	11.3	0.8	10.5	10.5
34	44	30	10	12.9	2.9	10.5	12.9	2.4	40	25	11	13.7	2.7	11	14	3	11.3	10.8
35	42	28	11	13.8	2.8	11	12	1	39	22	11.5	13.8	2.3	11.5	12.4	0.9	11.2	11.3
36	43	28	11	12.3	1.3	11	11.6	0.6	39	23	11	13.4	2.4	11	12	1	11.3	11.2
37	45	28	11	11.3	0.3	11	11.9	0.9	43	23	11	12	1	11	13	2	11.7	11.5
38	41	28	10.5	12.6	2.1	10	11.9	1.9	36	28	11.5	14	2.5	10.5	13.7	3.2	11.4	10.8
39	43	30	11	13.8	2.8	11	13.5	2.5	38	26	12	14.7	2.7	12	14.7	2.7	11.7	11.5
40	42	28	11	13.7	2.7	11	11.8	0.8	37	22	10.5	14.5	4	11	11	0	10.8	10.7
41	47	26	11.5	13.5	2	11	12.8	1.8	40	21	12	15.5	3.5	12	14.4	2.4	12	12

Appendix V Raw Data

Linear Dimensional Magnification

KEY: D=Mandibular R=Right L=Left M=Model 6=1st Molar
P=Panoramic Radiograph   N=Newtom

D/R 6-M	D/L 6-M	D/R 6-P	% Mag.	D/L 6-P	% Mag.	D/R 6-N	% Mag.	D/L 6-N	% Mag.
10.5	10.5	13.2	25.7%	11.6	10.5%	10.4	-1.0%	10.4	-1.0%
11	11	13.7	24.5%	13.1	19.1%	11.3	2.7%	11.3	2.7%
10.5	10.5	11.6	10.5%	11.7	11.4%	10.7	1.9%	10.7	1.9%
11	11	13.7	24.5%	13.4	21.8%	11	0.0%	11.3	2.7%
11	11	12.7	15.5%	11.3	2.7%	10.7	-2.7%	11	0.0%
11	11	13.8	25.5%	13.7	24.5%	11.3	2.7%	11.6	5.5%
11	11	13	18.2%	11.4	3.6%	11	0.0%	11	0.0%
11.5	11.5	14.2	23.5%	14	21.7%	11.3	-1.7%	11.9	3.5%
11	11	12.7	15.5%	14.5	31.8%	11.3	2.7%	11.3	2.7%
10	10	13.4	34.0%	11.4	14.0%	10.5	5.0%	10.5	5.0%
12	12	15.6	30.0%	14.2	18.3%	12.2	1.7%	12.2	1.7%
10	10	13.3	33.0%	10.8	8.0%	10.5	5.0%	10	0.0%
9.5	9.5	11.5	21.1%	10.8	13.7%	10.3	8.4%	10.2	7.4%
11.5	11.5	14	21.7%	14.1	22.6%	11.9	3.5%	11.6	0.9%
11	11.5	13.7	24.5%	13	18.2%	11	0.0%	11.3	-1.7%
10.5	9.5	11.5	9.5%	12	14.3%	10.5	0.0%	10	5.3%
11	12	14.5	31.8%	14.2	29.1%	12	9.1%	11.9	-0.8%
12	12	14.5	20.8%	14.9	24.2%	12.3	2.5%	12.5	4.2%
10.5	10.5	12.2	16.2%	12.2	16.2%	10.5	0.0%	10.5	0.0%
12	12	15.1	25.8%	15.9	32.5%	12.2	1.7%	12	0.0%
11	10.5	14.5	31.8%	12.3	11.8%	11	0.0%	10.5	0.0%
11.5	12	14.5	26.1%	14.5	26.1%	11.9	3.5%	11.8	-1.7%
10.5	10.5	13.3	26.7%	13.4	27.6%	10.5	0.0%	10.8	2.9%
11.5	11.5	14.4	25.2%	13.1	13.9%	11.5	0.0%	11.3	-1.7%
11	10.5	13.1	19.1%	14	27.3%	11.2	1.8%	11.2	6.7%
11.5	11.5	13.9	20.9%	13.2	14.8%	11.3	-1.7%	11.3	-1.7%
10.5	10.5	13.2	25.7%	11.3	7.6%	10.5	0.0%	10.5	0.0%
11	11	13.7	24.5%	14	27.3%	11.3	2.7%	10.8	-1.8%
11.5	11.5	13.8	20.0%	12.4	7.8%	11.2	-2.6%	11.3	-1.7%
11	11	13.4	21.8%	12	9.1%	11.3	2.7%	11.2	1.8%
11	11	12	9.1%	13	18.2%	11.7	6.4%	11.5	4.5%
11.5	10.5	14	21.7%	13.7	19.1%	11.4	-0.9%	10.8	2.9%
12	12	14.7	22.5%	14.7	22.5%	11.7	-2.5%	11.5	-4.2%
10.5	11	14.5	38.1%	11	4.8%	10.8	2.9%	10.7	-2.7%
12	12	15.5	29.2%	14.4	20.0%	12	0.0%	12	0.0%
Average Percentage			23.3%		17.6%		1.5%		1.2%

45